U.S. Coast Guard Research and Development Center
1082 Shennecossett Road, Groton, CT 06340-6048

Report No. CG-D-01-08

ANALYSIS OF BALLAST WATER SAMPLING PORT DESIGNS USING COMPUTATIONAL FLUID DYNAMICS

FINAL REPORT
February 2008

Prepared for:

U.S. Department of Homeland Security
United States Coast Guard
Washington, DC 20593-0001

N O T I C E

This document is disseminated under the sponsorship of the Department of Homeland Security in the interest of information exchange. The United States Government assumes no liability for its contents or use thereof.

The United States Government does not endorse products or manufacturers. Trade or manufacturers' names appear herein solely because they are considered essential to the object of this report.

This report does not constitute a standard, specification, or regulation.

James E. Fletcher
Chief, Safety and Response Consequence Management Branch
United States Coast Guard
Research & Development Center
1082 Shennecossett Road
Groton, CT 06340-6048

Technical Report Documentation Page

1. Report No.	2. Government Accession Number	3. Recipient's Catalog No.
CG-D-01-08		

4. Title and Subtitle	5. Report Date
Analysis of Ballast Water Sampling Port Designs Using Computational Fluid Dynamics	February 2008
	6. Performing Organization Code Project No. 4125
7. Author(s) R.V. Richard, J. F. Grant, E.J. Lemieux	8. Performing Report No. R&DC UDI # 780
9. Performing Organization Name and Address Naval Research Laboratory Bldg. F-14, Fleming Key Trumbo Annex Key West, FL. 33040 U.S. Coast Guard Research and Development Center 1082 Shennecossett Road Groton, CT 06340-6048	10. Work Unit No. (TRAIS)
	11. Contract or Grant No. HSCG32-06-XR00013
12. Sponsoring Organization Name and Address U.S. Department of Homeland Security United States Coast Guard Office of Operating and Environmental Standards Washington, DC 20593-0001	13. Type of Report & Period Covered Final
	14. Sponsoring Agency Code Commandant (G- 3PSO-4) U.S. Coast Guard Headquarters Washington, DC 20593-0001

15. Supplementary Notes

The R&D Center's technical point of contact is Penny Herring, 860-441-2868, email: penny.r.herring@uscg.mil.

16. Abstract (MAXIMUM 200 WORDS)

Analytical methods and computational fluid dynamics are used to describe flow conditions encountered at Naval Research Laboratory's Ballast Water Treatment Test Facility. Design tradeoffs are examined in the engineering of sample ports for collecting biological organisms in water samples, and criteria are provided for sample port installation in shipboard piping systems. Results of this work show that the ideal geometry for biological sampling is from the centerline of a straight, vertical, upward-flowing pipe having a sample port diameter between 1.5 and 2.0 times the basic isokinetic diameter as defined in this report. Sample ports should use ball valves for isolation purposes, and diaphragm or venturi valves for flow control; they should be located as close to the overboard outlet as possible; and they should be positioned as far from upstream obstructions and fittings as possible.

17. Key Words	18. Distribution Statement
ballast water, flow modeling, sample port, sample pipe, particle trajectory, isokinetic sampling	This document is available to the U.S. public through the National Technical Information Service, Springfield, VA 22161.

19. Security Class (This Report)	20. Security Class (This Page)	21. No of Pages	22. Price
UNCLASSIFIED	UNCLASSIFIED	62	

Form DOT F 1700.7 (8/72) Reproduction of form and completed page is authorized.

(This page intentionally left blank.)

EXECUTIVE SUMMARY

Ballast water is an inexpensive and efficient means for ships to maintain trim, counteract list, and adjust waterlines in response to cargo loading/unloading, or in response to foul weather. Ballast water is taken aboard as needed, stored in tanks, moved about, and discharged as required. In addition to the water itself, ballast water often contains organisms taken up with the water. The ballast water volume for any given ship can be tremendous—hundreds to tens or hundreds of thousands of metric tonnes. Frequently, ships ballast their tanks in one port and de-ballast them in another, with any entrained organisms being discharged with the ballast water. This practice has been identified as a vector for the translocation of non-indigenous species (NIS).

Under a joint effort between the United States Coast Guard (USCG) and the U.S. Environmental Protection Agency (EPA) Environmental Technology Verification (ETV) program, a draft ETV Protocol for the testing of commercial ballast water treatment technologies was created. This protocol calls for operational and challenge testing of commercial ballast water treatment equipment (BWTE). Likewise, the International Maritime Organization (IMO) has drafted standardized BWTE verification protocols through their G8 Guidelines. Both protocols require characterizing ballast uptake and treated discharge by way of collecting water samples during testing. The collection process for acquiring these samples must have minimal impact on living organisms within the ballast water, as these organisms are used to assess the efficacy of the BWTE. The organisms of interest are generally classified according to size ranges and include bacteria, phytoplankton, and zooplankton.

Under USCG sponsorship, a land-based facility was designed and constructed to evaluate the efficacy of BWTE in accordance with standardized protocols, including those protocols established in the ETV Program and in the IMO G8 Guidelines. The Ballast Water Treatment Test Facility (BWTTF) is a full-scale test stand, located at the U.S. Naval Research Laboratory (NRL) in Key West, FL, with capabilities for testing commercial BWTE using both ambient and surrogate organisms in accordance with the ETV test protocols. The monitoring and control capabilities at this facility provide an ideal environment for the design, modeling, and validation of biological sampling equipment and protocols unique to ballast water treatment testing.

This paper provides a review of analytical methods to describe flow conditions encountered in ballast systems. Several elements of ballast flow systems and the test facility are modeled using computational fluid dynamics. This modeling is augmented with an examination of the design tradeoffs in engineering sample ports for collecting biological organisms in water samples, as well as with recommendations for sample port installation criteria in shipboard piping systems. Results of the work show that the ideal geometry and location for biological sampling is from the centerline of a straight, vertical, upward-flowing pipe with a sample port diameter between 1.5 and 2.0 times the basic isokinetic diameter as defined in this report. Sample ports should use ball valves for isolation purposes and diaphragm or venturi valves for flow control; should be located as close to the overboard outlet as possible; and should be positioned as far from upstream obstructions and fittings as possible.

(This page intentionally left blank.)

TABLE OF CONTENTS

LIST OF FIGURES

LIST OF FIGURES (continued)

LIST OF TABLES

LIST OF ACRONYMS & SYMBOLS

#	Number
®	Registered trademark
A_p	Cross section area of ballast pipe
A_s	Cross section area of sample pipe
BWTE	Ballast water treatment equipment
BWTTF	Ballast Water Treatment Test Facility
Centipoise	Unit of viscosity (centimeter-gram-second)
CFD	Computational Fluid Dynamics
D	Inside pipe diameter
D_{ISO}	Isokinetic diameter
D_M	Main pipe sample diameter
e	Dissipation rate
E_{LL}	Entrance length (laminar)
E_{LT}	Entrance length (turbulent)
en, et	Velocity restitution coefficients
EPA	Environmental Protection Agency
ETV	Environmental Technology Verification Program
f	Friction factor
F	Fahrenheit
gpm	Gallons per minute
ID	Inside diameter
IMO	International Maritime Organization
in	Inch
K	Turbulent kinetic energy
kg	Kilogram
k-ε	Transport parameters for turbulent energy and its dissipation
L	Characteristic length
m	Meter
m^3/min	Cubic meters per minute
N	Newton

LIST OF ACRONYMS & SYMBOLS (continued)

NISA	National Invasive Species Act of 1996
NRL	Naval Research Laboratory
NRLKW	Naval Research Laboratory in Key West, Florida
OD	Outside diameter
Pa	Pascal
PC	Personal computer
psi	Pounds per square inch
PVC	Polyvinyl chloride
Q	Flow rate
$\mathbf{Q_{ISO}}$	Desired sample flow rate
$\mathbf{Q_M}$	Flow rate in main piping
$\mathbf{R_e}$	Reynolds number
$\mathbf{R_{e\ crit}}$	Critical Reynolds number
$\mathbf{R_{eL}}$	Reynolds number (laminar)
$\mathbf{R_{eT}}$	Reynolds number (turbulent)
s	Second
Schd 40	Schedule 40
TIFF	Tagged image file format
$\mathbf{T_l}$	Turbulent length
U.S.	United States
USCG	United States Coast Guard
v	Kinematic fluid viscosity, $v = \mu / \rho$
$\mathbf{v_{2,n}}$, $\mathbf{v_{2,t}}$	Reflection coefficients
Vs	Mean fluid velocity
μ	(Absolute) dynamic viscosity
ρ	Fluid density
$\mathbf{\rho_{sw}}$	Density of seawater

(This page intentionally left blank.)

1 INTRODUCTION

The transportation of non-indigenous species via ballast water and their deposition into coastal waters by way of ballast water is an ongoing problem. The current attempt to reduce the transportation of non-indigenous species by open-ocean ballast water exchange is a limited and interim solution. The National Invasive Species Act (NISA) of 1996 resulted in the United States Coast Guard (USCG) requiring vessels to implement ballast water management, which includes ballast water exchange or treatment. More stringent regulations are anticipated for ballast water treatment by the USCG, the International Maritime Organization (IMO), and possibly other domestic regulators in the near future. These regulations will likely result in the need for onboard ballast water treatment to kill, remove, or otherwise inactivate organisms within the ballast water.

With support from and in partnership with the USCG, the Naval Research Laboratory Key West (NRLKW) has designed and constructed, and currently operates, the Ballast Water Treatment Test Facility (BWTTF). The BWTTF is used to evaluate the efficacy of Ballast Water Treatment Equipment (BWTE) in accordance with standardized protocols, including those protocols established in the Environmental Protection Agency's (EPA) Environmental Technology Verification (ETV) Program, and in the International Maritime Organization's G8 Guidelines. The objectives of this unique facility are to provide third-party independent and objective testing of BWTE, and to provide data from standardized tests to other entities for certification.

During the development of the BWTTF, significant effort was spent to characterize the mechanical methods for injecting and sampling biological organisms into and from ballast water flow streams. As a result of these efforts and ongoing testing at the BWTTF, it was recognized that: (1) sample port design for collecting and detecting biological organisms in ballast water was not well characterized; and (2) the BWTTF provided an ideal platform for modeling, characterizing, and establishing design criteria for sampling systems (sampling pipes, ports, or wands) that can be applied to compliance testing in the shipboard environment. The intent of this report is to characterize flow regimes typical of ballast water systems; to model various sampling port designs using classical fluid mechanics as well as computational fluid dynamics (CFD) techniques; and to provide recommendations for shipboard sample port design.

2 OBJECTIVE

The objective of this research was to establish a sound fluid mechanics basis for the design of sampling ports to be used in shipboard sampling of ballast water discharge. Emphasis was placed on obtaining a representative sample of ballast water discharge, while minimizing any adverse effects on organisms, in an effort to generate a set of design and installation guidelines for ballast water sampling ports.

3 TECHNICAL APPROACH

The technical approach of this effort was to characterize flow conditions and biological organism response under various piping and sampling configurations, using both classical fluid mechanics techniques and computational fluid dynamics (CFD) analysis. By characterizing the flow in this way, it was expected that a set of guidelines for the geometry and sizing of sampling systems could be developed to ensure that samples collected were representative of the number of organisms present, while minimizing mortality and organism damage due to sampling.

Initial analyses were based on modeling existing piping and pumps at NRLKW. The results of these analyses were used to recommend design guidelines for typical shipboard arrangements. These guidelines were then used to design and analyze sample wand requirements for a known shipboard ballast water system.

3.1 Classical Fluid Mechanics Analysis

Fluid flow in pipes is a well-understood physical phenomenon, with the fundamental properties of flow in pipes being characterized by the Reynolds number. The Reynolds number quantifies the relative importance of inertial and viscous forces for a given set of flow conditions (see Equation 1), and is used to identify particular flow regimes, such as laminar or turbulent flow.

$$R_e = \frac{\rho \upsilon_s^2 / L}{\mu \upsilon_s / L^2} = \frac{\rho \upsilon_s L}{\mu} = \frac{\upsilon_s L}{\nu} = \frac{\text{Inertial forces}}{\text{Viscous forces}} \qquad \textbf{Equation 1}$$

where:

υ_s = mean fluid velocity [m s^{-1}]
L = characteristic length [m]
μ = (absolute) dynamic fluid viscosity [N s m^{-2}] or [Pa s]
ν = kinematic fluid viscosity: $\nu = \mu / \rho$, [m^2 s^{-1}]
ρ = fluid density [kg m^{-3}]

For flow in a circular cross-section pipe, the characteristic length (L) is the pipe diameter.

Laminar flow occurs at low Reynolds numbers, where viscous forces are dominant, and is characterized by smooth, constant fluid motion. Turbulent flow occurs at high Reynolds numbers and is dominated by inertial forces, which produce random eddies, vortices, and other flow fluctuations.

The transition between laminar and turbulent flow occurs at a critical Reynolds number: ($R_{e\ crit}$). For smooth-walled circular pipes, the critical Reynolds number is generally accepted to be 2000. Within a certain range around this point, there is a transition region where the flow is neither fully laminar nor fully turbulent and predictions of fluid behavior can be difficult. For smooth-walled circular pipe flow with a Reynolds number above 4000 the flow is fully turbulent.

Representative velocity profiles for laminar and turbulent flows are shown in Figure 1. Laminar velocity profiles are parabolic, with the average velocity generally assumed to be one half the parabola's height. Turbulent profiles are much more uniform across the pipe cross-section, with the average velocity generally assumed to be the centerline velocity.

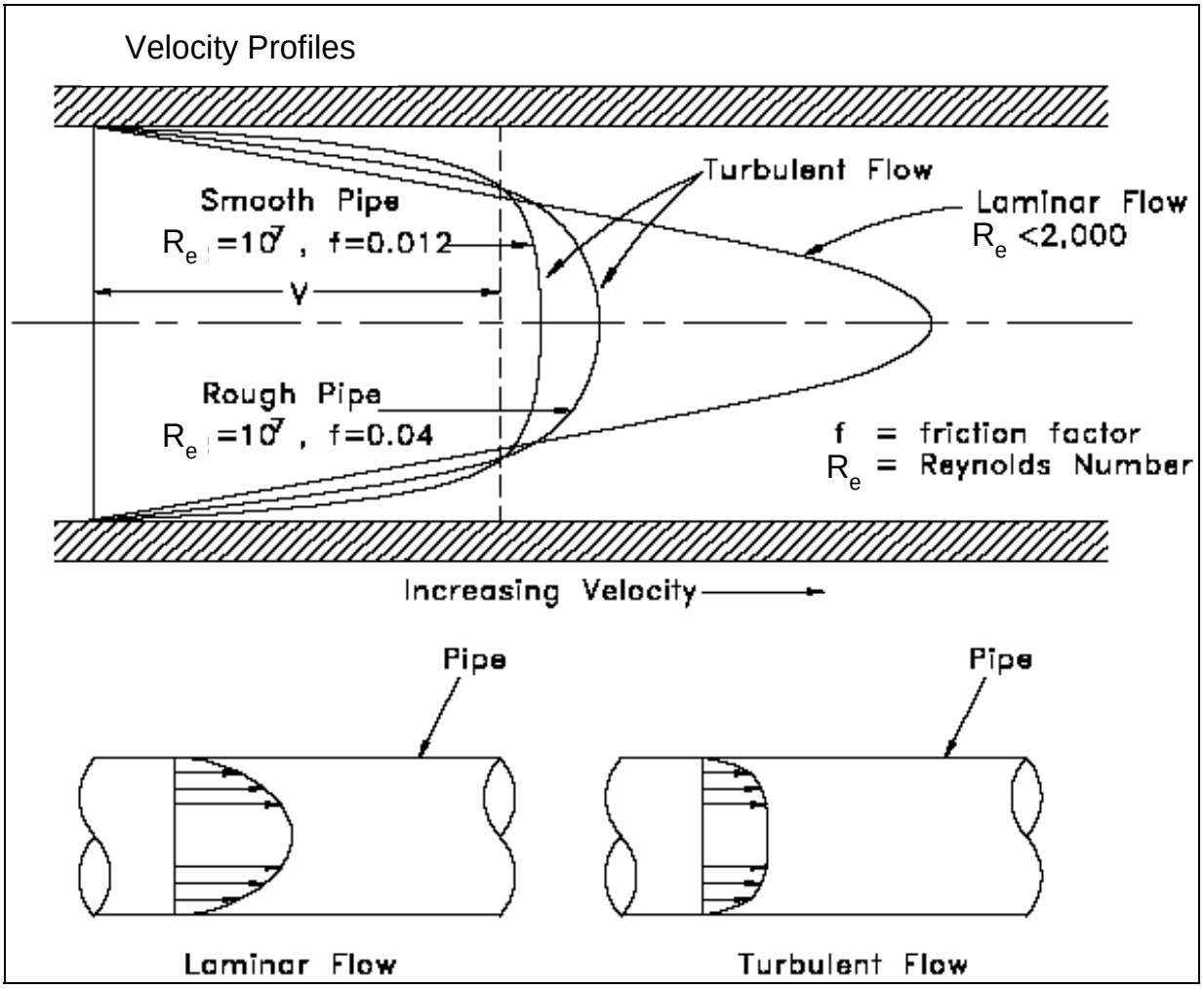

Figure 1. Laminar and turbulent velocity profiles.

The entrance length is the distance required to establish a fully developed velocity profile following flow through a bend, pump, valve, or the like, and is used as a parameter to position sensors and ports in a region of fully developed flow. This length can be expressed dimensionlessly as the number of pipe diameters required to allow fully developed flow as a function of Reynolds number, as shown in the following equations:

For laminar flow, the entrance length is defined as:

$$E_{LL} = .06\, R_{eL} \qquad \textbf{Equation 2}$$

At the limit of laminar flow ($R_{eL} = 2000$), the entrance length is:

$E_{LL} = 120$ diameters.

For turbulent flow, the entrance length is given by:

$$E_{LT} = 4.4\, R_{eT}^{\frac{1}{6}} \qquad \textbf{Equation 3}$$

At the onset of fully turbulent flow ($R_{eT} = 4000$), the entrance length is:

$E_{LT} = 17.5$ diameters.

3.1.1 Properties of Sea Water

In order to characterize the flow for ballast water sampling, calculations should be based on the fluid dynamic properties of typical seawater. The physical properties used throughout this study for seawater are as indicated in Table 1. The dynamic viscosity is listed in the table in Centipoise, where 1000 Centipoise equals 1 Pascal-second. For the calculation of basic flow characteristics, a temperature of 70 degrees Fahrenheit (F) was chosen as being typical of the seawater temperature at the BWTTF in Key West.

Table 1. Density and dynamic viscosity of seawater for various temperatures.

	DENSITY OF SEA WATER	VISCOSITY OF SEA WATER
Temperature (degrees F)	Pounds percubic foot	Centipoise
30	64.25	1.88
40	64.2	1.61
50	64.17	1.4
60	64.1	1.21
70	64.02	1.06
80	63.95	0.92
90	63.8	0.815
100	63.7	0.73

3.1.2 Basic Flow Calculations

Fundamental flow parameters for the configurations of interest were calculated using conventional fluid dynamic analysis. These parameters included average flow velocity and Reynolds number for given pipe diameters, fluid properties, and flow rates. Table 2 provides definitions for MathCAD® calculations of the basic parameters. Typical results for the BWTTF main piping and sample flows are shown in Table 3. The key conclusion here is that these flows are well beyond the laminar range, indicating that all of the sampling would be done in fully turbulent flows.

Table 2. MathCAD® definitions for basic flow parameters.

Ballast Water Sampling NRL Test System
Basic Flow Parameters

Main Piping:

8 inch Schd 40 PVC Pipe $ID = 7.981\,in$ $OD = 8.625\,in$

$A_p = \frac{\pi \cdot ID^2}{4}$ $A_p = 50\,in^2$ Where Ap is the cross sectional area of the pipe

Assume Pipe to be Smooth

Main Piping Flow Characteristics:

Sea Water	Density	$\rho_{sw} = 64.02\,\frac{lb}{ft^3}$	$\rho_{sw} = 1026\frac{kg}{m^3}$
Dynamic Viscosity		$\mu = 1.06\,centipoise$	$\mu = 1.06\times 10^{-3}\,\frac{kg}{ms}$
Kinematic Viscosity		$\nu = \frac{\mu}{\rho_{sw}}$	$\nu = 1.034\times 10^{-6}\,\frac{m^2}{s}$
Nominal Flow Rate		$Q_{sw} = 5085\,\frac{in^3}{sec}$	$Q_{sw} = 300\,\frac{m^3}{hr}$
Average Velocity		$V_{sw} = \frac{Q_{sw}}{A_p}$	$V_{sw} = 101.7\frac{in}{sec}$
Reynolds Number		$R_{esw} = \frac{ID \cdot V_{sw}}{\nu}$	$R_{esw} = 5.1\times 10^5$

Reynolds Number > 4000 Flow is Fully Turbulent

Table 3. Typical flow parameters for sample piping at the BWTTF.

Sample Piping

1 ½ in. Schd 40 PVC $ID_S = 1.61\,in$ $OD_S = 1.90\,in$

$A_S = \frac{\pi \cdot ID_S^{\,2}}{4}$ $A_S = 2\,in^2$ Where As is the cross sectional area of the sample pipe

Nominal Flow Rate, Q $Q_S = 3\frac{m^3}{hr}$ $Q_S = 51\frac{in^3}{sec}$ $Q_S = 13.2\frac{gal}{min}$

Average Velocity, V $V_S = \frac{Q_S}{A_S}$ $V_S = 25\frac{in}{sec}$

Reynolds Number $R_{es} = \frac{ID_S \cdot V_S}{\nu}$ $R_{es} = 3 \times 10^4$

Reynolds Number > 4000 Flow is Fully Turbulent

3.2 Computational Fluid Dynamics Analysis

3.2.1 Computational fluid dynamics (CFD)

CFD is one of the branches of fluid mechanics that uses numerical methods and algorithms to solve and analyze problems that involve fluid flows. Computers are used to perform the millions of calculations required to simulate the interaction between fluids or gases and the complex surfaces used in engineering. To study the fluid flow for ballast water sample piping, the commercial application COSMOSFloWorks® was used. COSMOSFloWorks® (FloWorks®) is an analysis package integrated with the SolidWorks® design and solids modeling software. FloWorks® was developed as an engineering analysis and design tool rather than as an open-ended R&D software package.

Using commercial software places limits on tailoring algorithms beyond the scope of the software. However, COSMOSFloWorks® is a robust package with extensive capabilities, and its integration with SolidWorks® facilitates rapid model generation and easy modification of geometry, fluid types, and boundary or initial conditions.

Although primarily a tool of the design engineer, FloWorks® has extensive modeling and analysis capabilities for studying a wide range of fluid flow and heat transfer phenomena, including the following, which are relevant to this effort:

- External and internal fluid flows
- Compressible gas and incompressible fluid flows
- Free, forced, and mixed convection
- Fluid flows with boundary layers, including wall-roughness effects
- Laminar and turbulent fluid flows
- Multi-species fluids and multi-component solids
- Flows of compressible liquids
- Two-phase (fluid + particles) flows

COSMOSFloWorks® solves Navier-Stokes equations, which are formulations of mass, momentum, and energy conservation laws for fluid flows. These equations are supplemented by fluid state equations that define the nature of a fluid, and by empirical dependencies of fluid viscosity and/or thermal conductivity on temperature. A particular problem is finally specified by the definition of its geometry and its boundary and initial conditions.

Most of the fluid flows encountered in engineering are turbulent, so COSMOSFloWorks® was mainly developed to simulate and study turbulent flows, by way of employing a single system of equations to describe both laminar and turbulent flows. Moreover, transition from a laminar to turbulent state, and/or vice versa, is possible. To predict turbulent flows, COSMOSFloWorks® uses the Reynolds-averaged Navier-Stokes equations, where time-averaged effects of the flow turbulence on the flow parameters are considered, whereas the other (large-scale, time-dependent) phenomena are taken into account directly. Through this procedure, extra terms known as the Reynolds stresses appear in the equations, for which additional information must be provided. To close this system of equations, COSMOSFloWorks® employs transport equations for turbulent kinetic energy and its dissipation rate: the so-called k-ε model (COSMOSFloWorks® Fundamentals Manual, 2005).

3.2.1.1 The Turbulent Length Scale

The turbulence length scale is a physical quantity that describes the size of the large energy-containing eddies in a turbulent flow. For fully developed turbulent pipe flow, the turbulent length can be shown to be:

$$T_l = .07*D \qquad \textbf{Equation 4}$$

where D = pipe inside diameter

The turbulent length scale is often used to estimate the turbulent properties at the inlets of a CFD simulation. Because the turbulent length scale is a quantity that is intuitively easy to relate to the physical size of the problem, it is easy to estimate a reasonable value of the turbulent length scale. The turbulent length scale should normally not be larger than the dimensional boundaries of the CFD model; otherwise, the turbulent eddies would be larger than the problem size.

3.2.1.2 Two-Phase (Fluid + Particles) Flows

COSMOSFloWorks® calculates two-phase flows as a motion of spherical liquid particles (droplets), or spherical solid particles, in a steady-state flow field. COSMOSFloWorks® can simulate dilute two-phase flows only where the influence of a particle on the fluid flow (including temperature) is negligible (for example, flows of gases or liquids contaminated with particles). These are the cases where the particles' mass flow rate fraction is lower than about 30 percent of the mixture mass flow rate.

The particles of a specified (liquid or solid) material and constant mass are assumed to be spherical. COSMOSFloWorks® calculates the drag coefficient with Henderson's formula derived for continuum and rarefied; subsonic and supersonic; laminar; transient; and turbulent flows over the particles (Henderson, 1976). Particle interaction with the model surfaces is taken into account by specifying the particle's full absorption (typical for liquid droplets impinging on surfaces at low or moderate velocities), or by its ideal or non-ideal reflection (typical for solid particles).

For the modeling of ballast water sampling, COSMOSFloWorks' internal flow analysis of turbulent two-phase flows was used to investigate the injection and sampling of biological organisms for NRL's BWTTF as well as for typical shipboard systems. All of the flows modeled were inside pipes and therefore internal. The two-phase flow capabilities allowed for analyzing the flow of particles representing the biological particles (or organisms) within the flow field.

3.3 Isokinetic Sampling

Sampling a flow stream requires extracting a portion of the flow stream through a sample port. Ideally, this sample port is configured to obtain a representative sample, or a sample that is consistent with the composition of the overall flow stream. In sampling biological organisms, the sample needs to contain the same ratio of live and dead organisms as the main flow stream contains and should induce no additional mortality of biological organisms. Typically, the total sample volume is obtained over a time interval during a flow event, so that a time-integrated sample is collected to reflect any normally occurring density variations.

Various types of sampling methods were examined in this effort. Depending on pipe diameters and other external factors, the flow velocities in the sample stream were seen to be greater or less than the velocities in the main ballast pipe. Isokinetic sampling is a special case, where the two velocities are equal by design; that is, the velocity profile at the sample port matches the velocity profile in the main stream (Fish, 1997). Isokinetic sampling is most often used when sampling for constituents that, because of significantly different flow properties, tend to separate due to changes in the flow field. Such constituents include oil/water mixtures, where the non-immiscible constituents can separate due to changes in velocity, thereby biasing the concentrations in the sample. Separation can also occur when sampling for particles having significantly different densities than the carrier liquid has.

Because many of the organisms being sampled in ballast water have densities similar to that of the water, the strict requirement for isokinetic sampling is unnecessary. However, the isokinetic diameter for a straight-tube sampler is of interest and will be seen to be useful as a design guideline for sampler sizing.

For turbulent pipe flows, true isokinetic sampling is virtually impossible to implement, due to the high variability and constant fluctuations in instantaneous flow. Furthermore, highly turbulent flows have significantly long entrance lengths that require long straight sections to fully develop. However, using the mean flow, a simple theoretical model for isokinetic sample tube diameter can be derived. Figure 2 presents the basic definitions used in isokinetic calculations.

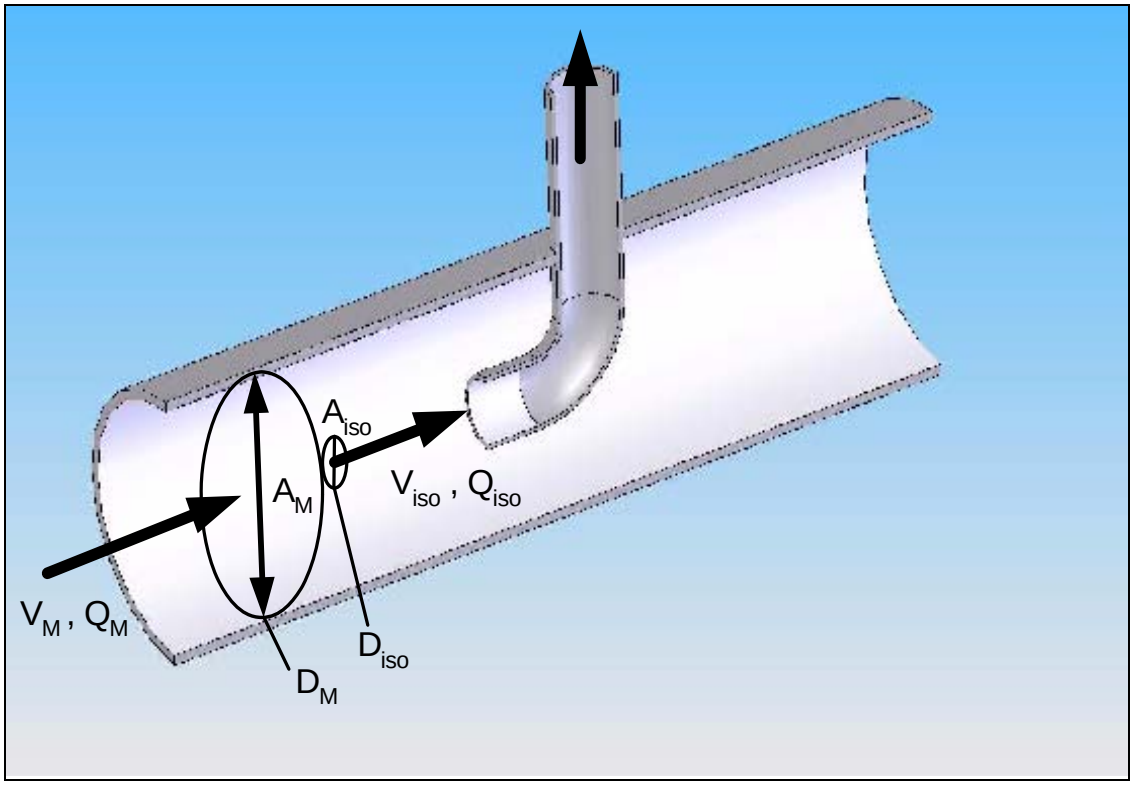

Figure 2. Isokinetic parameters.

If one makes the often-used assumption that the centerline velocity for turbulent flow is equal to the average velocity, then the isokinetic sample diameter (D_{iso}) can be derived as follows:

$$D_{iso} = D_M \sqrt{\frac{Q_{iso}}{Q_M}} \qquad \textbf{Equation 5}$$

where:

D_M = main pipe diameter

Q_M = flow rate in the main piping

Q_{iso} = desired sample flow rate

To investigate the effect of sample port diameter and isokinetic sampling on sample flow trajectories, the model shown in Figure 3 was used. The figure shows the boundary conditions for the simulations as well as the fully developed velocity profile in the main pipe. Simulations for sample port diameters equal to, less than, and greater than the isokinetic diameter were performed. The simulations take advantage of the symmetry of the system, by modeling only one quarter of the pipe, to reduce computation time.

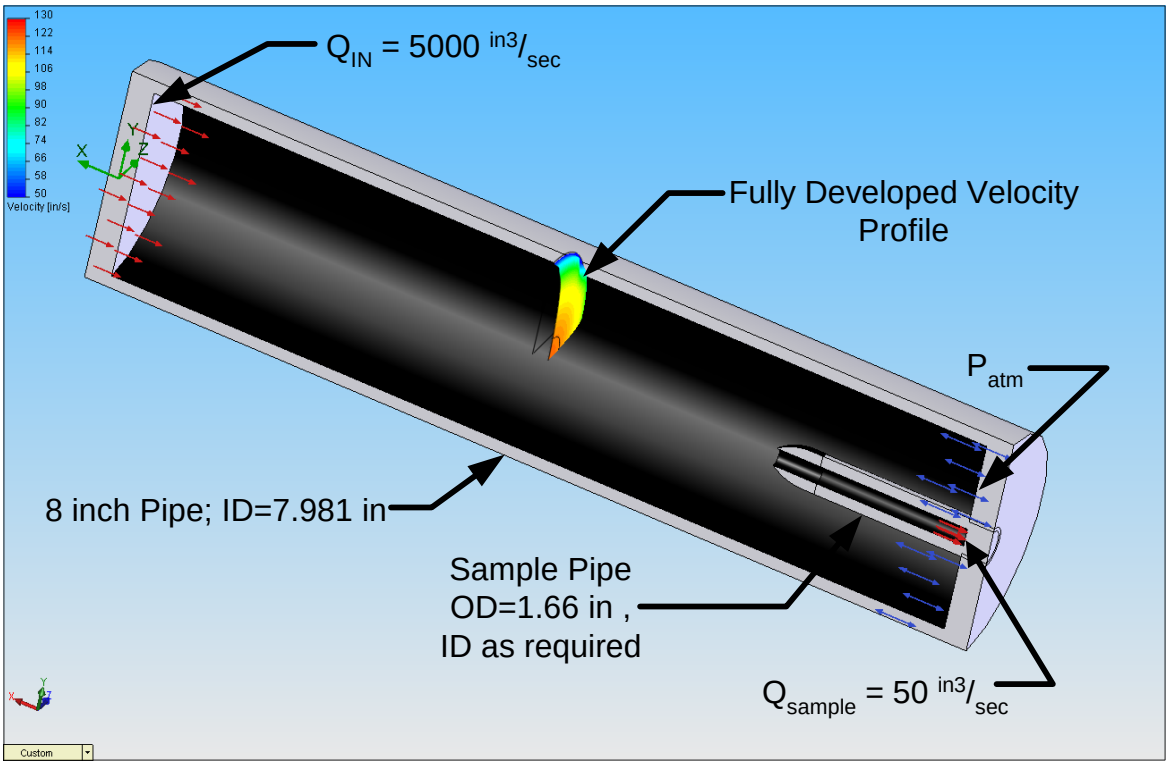

Figure 3. Model geometry, boundary conditions and main pipe velocity profile for isokinetic sampling investigations.

3.3.1 Isokinetic Diameter Simulations

The first isokinetic simulation was run with the diameter calculated using Equation 5 and the values defined in Figure 3. Thus:

$$D_{iso} = 7.98\ \text{in}\sqrt{\frac{50\frac{\text{in}^3}{\text{sec}}}{5000\frac{\text{in}^3}{\text{sec}}}} \qquad D_{iso} = 0.798\ \text{in}$$

The average velocity for these conditions, and thus the isokinetic velocity, is:

$$V_{iso} = 100 \frac{in}{sec}$$

Figure 4 shows the flow trajectories (colored to indicate velocity) entering the sample port for this simulation. (Again, because of the inherent symmetry, the calculations are performed for only ¼ the pipe diameter to reduce calculation time.) The end of the probe is tapered in a bullet-nose shape to minimize any effects that stalling against a blunt nose might impose on the downstream flow. The calculated velocity for the centerline flow in the main pipe is 119 in/sec, which is 19 percent higher than the isokinetic prediction. This result was expected, because the isokinetic velocity formulation was based on the assumption that the centerline velocity was equal to the average velocity, when in fact there is a slightly curved velocity profile with a maximum at the centerline.

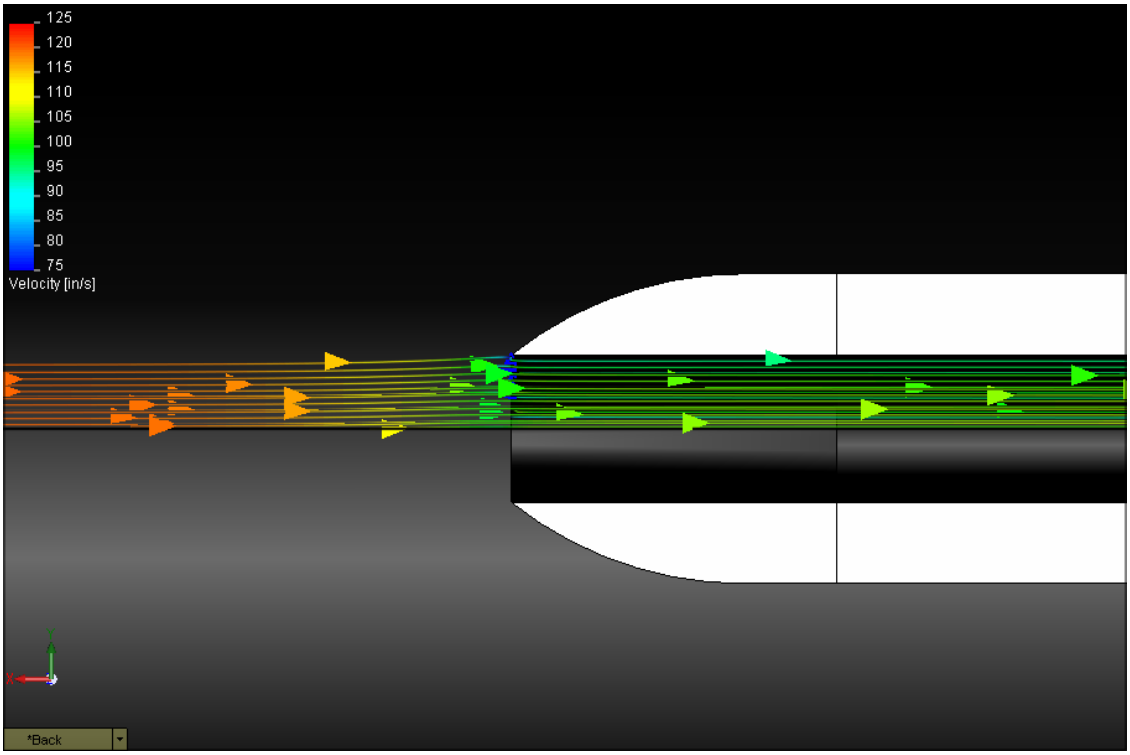

Figure 4. Preliminary isokinetic diameter flow trajectories.

The theoretical velocity at the centerline of the pipe is given by:

$$V_{max} = V_{av}\left(1 + 1.43\ f^{\frac{1}{2}}\right) \qquad \textbf{Equation 6}$$

where f is the friction factor, and is a function of the Reynolds number:

$$f = \frac{1.325}{\left(\ln\left(\frac{e}{3.7D} + \frac{5.74}{(R_e)^9}\right)\right)^2}$$ **Equation 7**

For the current simulation, the Reynolds number is:

$$R_e = 5.1 \times 10^5$$

yielding a friction factor (f) of 0.013.

The resulting centerline velocity, calculated with Equation 6, is 116 in/sec. This result represents a 2.5 percent discrepancy between the theoretical calculation and the CFD results, which is most likely due to computational error, but which is well within acceptable results.

The theoretical isokinetic diameter for this adjusted centerline velocity can be shown to be:

$$v_r = \frac{1}{1 + 1.43\sqrt{f}}$$ **Equation 8**

where:

$$D_{iso} = D_M \sqrt{\frac{Q_{iso} * v_r}{Q_M}}$$ **Equation 9**

Thus, the adjusted isokinetic diameter for the above simulation is:

$$D_{iso} = 0.74 \text{ in}$$

Figure 5 shows a plot of the flow trajectories for this revised diameter calculation as a function of velocity. The difficulties in trying to match isokinetic sampling conditions become apparent in this simulation. There is a slight slowing of the flow field in front of the sample port due to an increase in pressure as the flow field adjusts to the changing velocity profile in the sample port. Although the average velocity in the sample flow is very close to the main centerline velocity, the flow is forced to readjust by attaching to the wall and establishing a new turbulent profile.

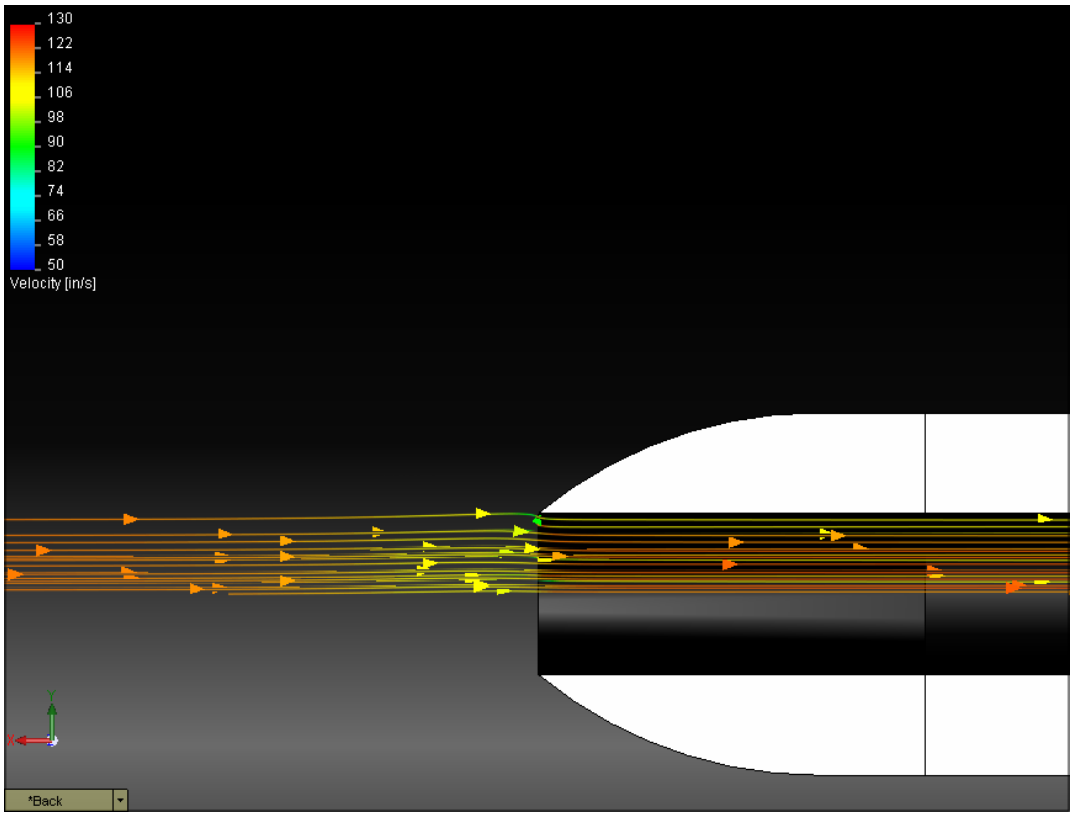

Figure 5. Sample trajectories for revised isokinetic diameter.

Clearly, there is no justification for trying to calculate an exact isokinetic diameter. For the studies regarding sample diameter, the isokinetic diameter calculated with Equation 5 will be used.

Figure 6 presents flow trajectories for a sample port having a diameter of 0.5 inches, which is 62 percent of the basic isokinetic diameter. This simulation clearly shows the potential problem with sampling through a port that is smaller than the isokinetic diameter. The sample is extracted from the same core diameter in the main flow but is forced to accelerate as it enters the sample port and as the outer flow trajectories are forced to suddenly turn into the sampler. This dynamic greatly increases the likelihood of particles impacting the tip of the sample wand, and would tend to separate out particles having a density higher than that of seawater.

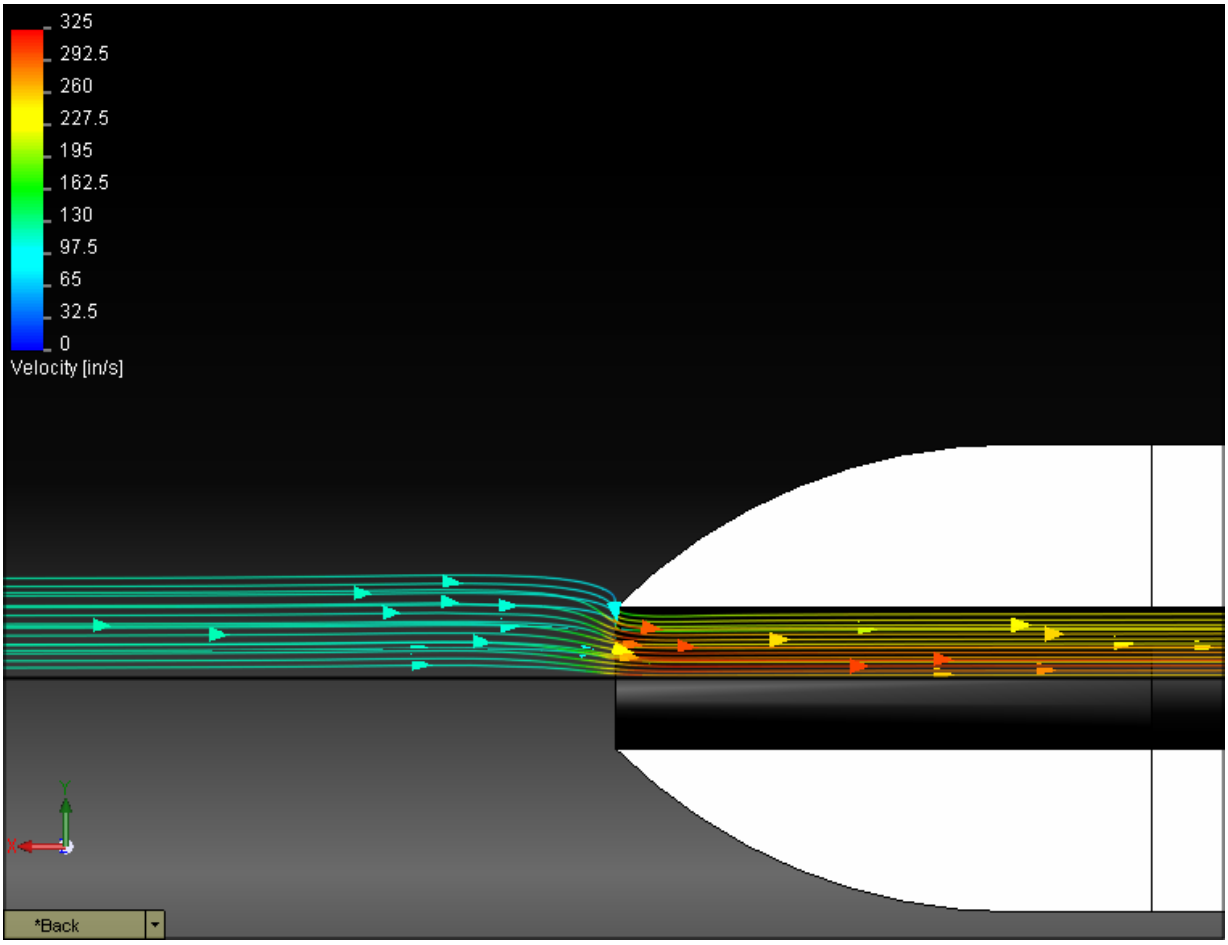

Figure 6. Flow trajectories colored to indicate velocity for 62 percent isokinetic diameter.

The increased velocity in the sample wand, which would lead to higher turbulence and increased mortality, also results in a pressure decrease in the sample wand. This phenomenon is a classic example of Bernoulli's Principle: In order to maintain energy balance if the velocity in a flow increases, the pressure must decrease. This relationship is shown in Figure 7, which plots the pressure across the wand exit. The average pressure across this section is 10 psi, which is almost 5 psi below the main pipe pressure. Because most sampling systems will take samples close to the overboard outlet, the main pipe pressure at the sampling port will be close to atmospheric pressure. For this simulation, the pressure drop is only 0.025 psi/ft; therefore, even sampling 10 feet from the discharge would only increase the pressure by 0.25 psi.

Therefore, this sampler would require a pump to establish the necessary pressure drop to induce the desired flow rate. Decreasing the diameter further can very quickly lead to a situation where the desired flow rate cannot be achieved by an external pump that, at most, could reduce the pressure by 14.7 psi.

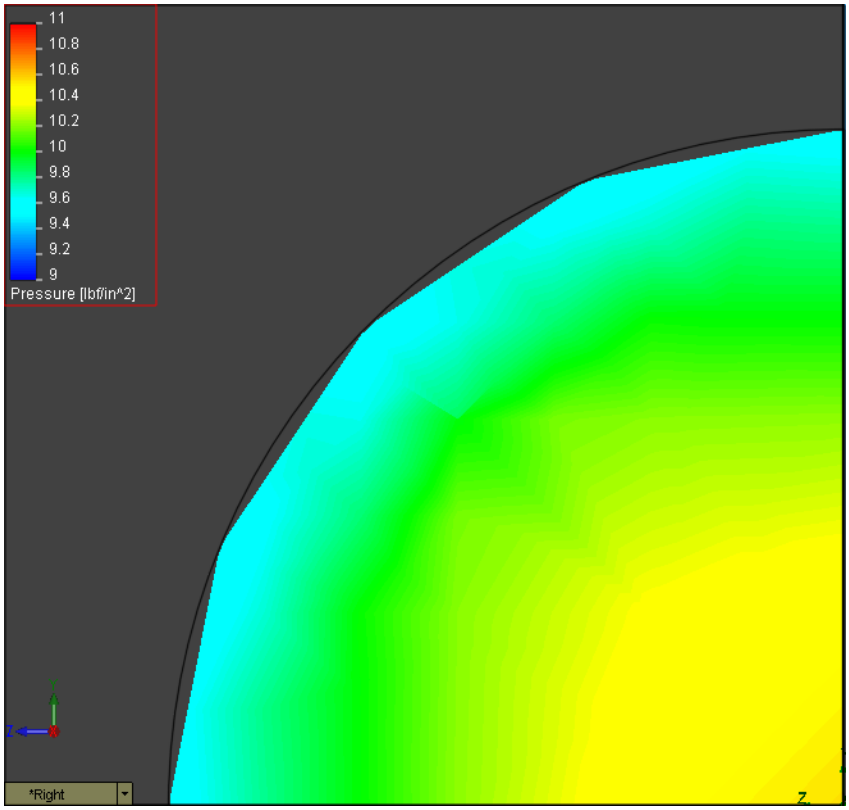

Figure 7. Sample port exit pressure for 62 percent isokinetic diameter.

Next, consider sampling through a port 1.38 inches in diameter, which is the inside diameter of a 1¼-inch nominal standard Schedule 40 pipe. This diameter is 1.72 times the basic isokinetic diameter. The flow trajectories as a function of velocity are shown in Figure 8. The transition from the main flow to the sampler is essentially the same as that for an elbow simulation as seen later in Section 4.1.2.3. The transition occurs in less than one sample port diameter. This brief interval should minimize any separation of constituents and therefore come closest of any of the samplers modeled to meeting the intent of isokinetic sampling.

Sampling with a port significantly larger than the isokinetic diameter has several advantages. First, the transition into the pipe is smooth, and the reduced velocity in the sample line would reduce biological mortality due to sampling. Second, the pressure increase in the sample line means that no pumping would be required to extract a sample at the desired flow rate. Third, moderate changes in the main flow or sample rate would not change the fundamental character of the sample flow and transition.

These advantages suggest that a sample port diameter of at least 1.5 times the calculated isokinetic diameter should be used. Regarding larger ratios, Figure 9 shows flow trajectories for a sample port diameter three times the isokinetic diameter. This port appears to be too large for good sampling. The flow trajectories show that a significant backflow must occur around the inside of the sample probe, extending inside about ¼ in.

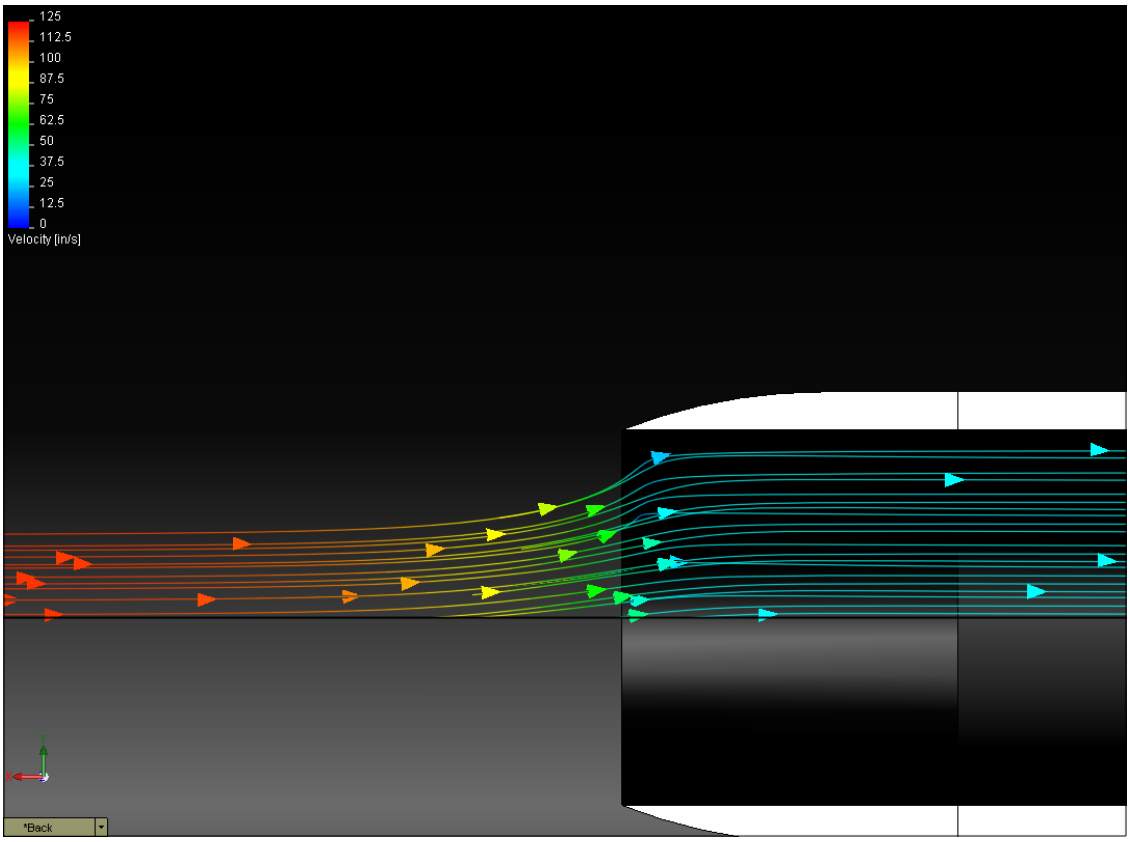

Figure 8. Flow trajectories for a 172 percent isokinetic diameter sample wand.

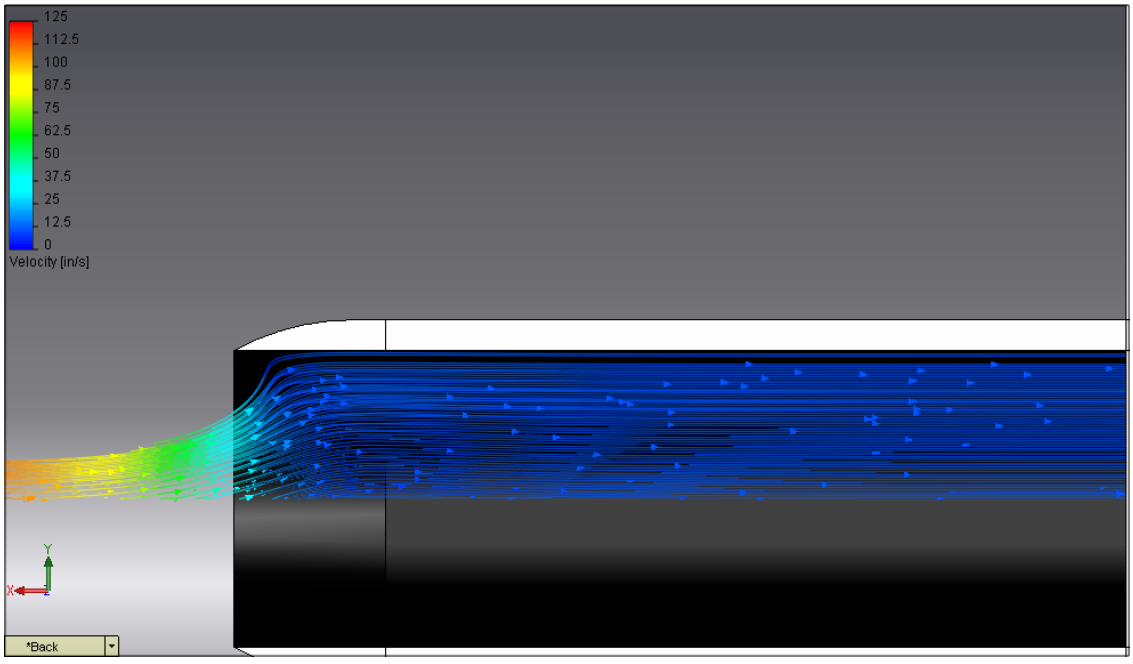

Figure 9. Flow trajectories for a 3X isokinetic diameter sample wand.

This backflow is seen more clearly in Figure 10, which shows velocity trajectories in the inlet region. This region would become even more chaotic if turbulent eddies were included in the figure. Thus, the likelihood of capturing particles that interact severely with the sampler wall (and thereby increase mortality) would be increased. The examination of sample pipe diameters identified that optimal flow characteristics with minimal mortality occur when the diameter is 1.5 to 2.0 times the mean isokinetic diameter, D_{iso}.

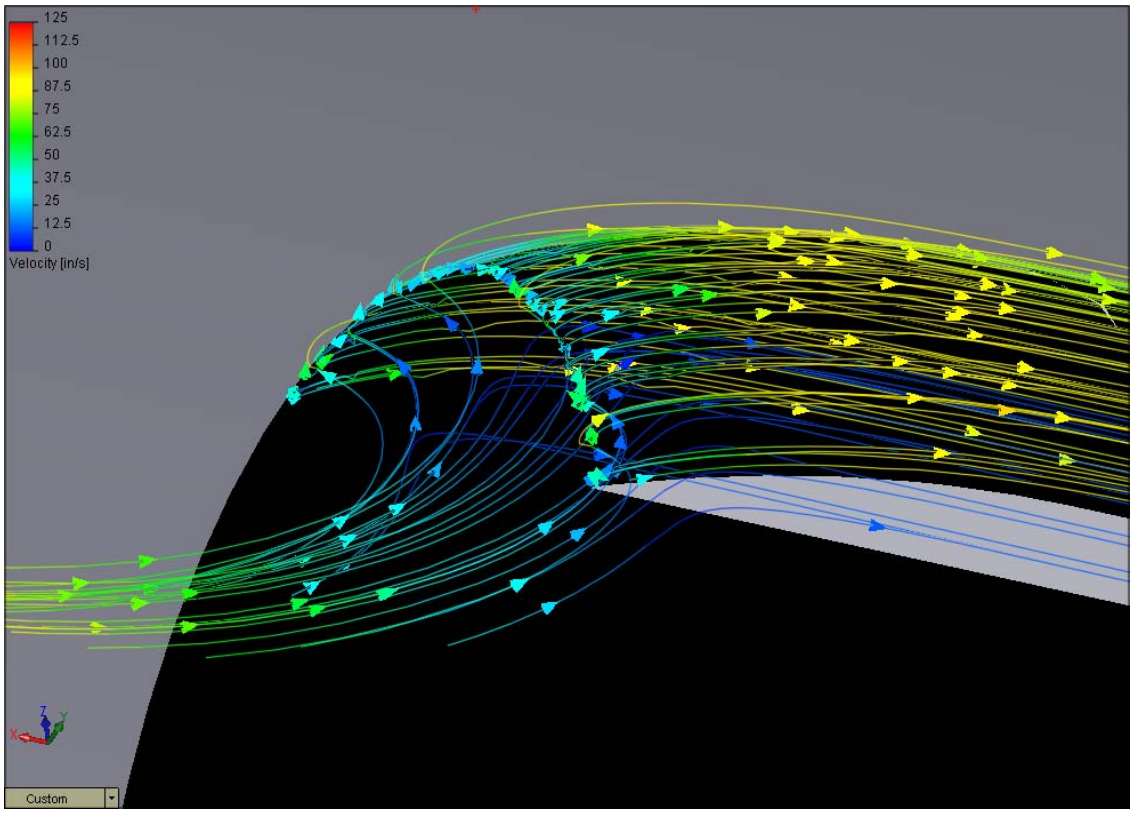

Figure 10. Flow trajectories near entrance of a 3X isokinetic diameter sampler.

3.4 Ballast Water Treatment Test Facility

The BWTTF is located on Fleming Key at Trumbo Point Annex, Naval Air Station Key West, FL. The main mixing loop on the transfer skid, shown in Figure 11, is part of the Naval Research Laboratory Center for Corrosion Science and Engineering. The BWTTF functions as a scientific test platform for assessing technologies designed to eliminate aquatic nuisance species in shipboard ballast water.

Figure 11. BWTTF injection piping layout.

To allow differentiation between treatment technologies, verification testing is conducted so that comparable information is available to consumers and other stakeholders. The use of a land-based facility incorporating a standard set of challenge conditions provides comparable and defensible results. The BWTTF is designed specifically to perform ETV verification testing, and is a fully instrumented seawater storage and transfer system that replicates the volumes, flows, and pressures typical of systems on marine vessels. Evaluations of candidate ballast water treatment technologies are performed in accordance with the facility test plan, which is based on the "Generic ETV Protocol for the Verification of Ballast Water Treatment Technologies", currently in final draft.

BWTTF pumps can provide flow rates up to 1350 gpm (5.1 m^3/min); BWTTF tanks include a 101,000-gallon (382 m^3) test ballast tank, a 40,000 (151 m^3)-gallon control test tank, and a 104,000 (394 m^3)-gallon discharge tank. The facility provides means for injecting specified test organisms, as well as for monitoring test conditions, sampling, and laboratory analysis. All water from testing is treated prior to final discharge to remove all added challenge components and any by-products of the treatment system. To accommodate as yet undefined/unidentified technologies for testing, the system can be reconfigured to accommodate treatment systems that operate under any combination of ballast uptake, in-tank storage, or ballast discharge.

3.5 Shipboard Systems Analysis

Defining the characteristics of a typical shipboard ballast water system suitable for the design of a ballast water sampling system is problematic. The details of the pumping and piping systems vary significantly, even within a single class of ship. Ballast water discharge can vary considerably, even for a single ship depending on the ballast requirements for a particular cargo.

In order to begin to bound the problem, data for ballast storage volumes, USCG correspondence, and internet searches were used to obtain information on typical pipe sizes and pump capacities for several classes of ships. These data were used to generate the parameters shown in Table 4. Calculations of the maximum flow rates were based on a pipe diameter of 20 inches, and on a maximum pump discharge of 3000 cubic meters per hour. A three cubic meter sample size is called out by the draft ETV protocol and equates to about 800 gallons.

Table 4. Typical shipboard ballast water system parameters.

	Max Allowable Vel	4 m/s								
	Single Pump Flow	3000 m^3/hr								
	Ship	Max. Pump (m^3/hr)	Max. No. Pumps Req.	Max Pump Pipe Flow Rate (m^3/hr)	Pipe max (in)	Max. Vel. (m/s)	Volume (m^3)	Max. Pump Out Time (hr)	Flow (GPM) For 1 cu. m sample	Flow (GPM) For 1 cu. m sample
Replace Cargo	Dry Bulk Carrier	10,000	4.0	2,500.0	20	3	20,275	4.1	3.3	6.5
	Ore Carriers	10,000	4.0	2,500.0	20	3	20,275	2.0	6.5	6.5
Return Empty	Bulk Oil Carrier	20,000	7.0	2,857.1	20	4	66,522	6.7	2.0	4.0
	Liquid Gas Carrier	10,000	4.0	2,500.0	20	3	31,000	6.2	2.1	4.3
	Oil-Bulk-Ore	15,000	5.0	3,000.0	20	4	31,000	3.1	4.3	6.4
Ship Control	Container Ship	2,000	1.0	2,000.0	20	3	6,920	6.9	1.9	3.8
	General Cargo	2,000	1.0	2,000.0	20	3	6,920	6.9	1.9	3.8
	RO-RO	2,000	1.0	2,000.0	20	3	6,920	6.9	1.9	3.8

The number of discharge pumps required was determined by setting the maximum allowable velocity to 4 meters per second, while requiring an integer number of pumps. A pump out time was then calculated, and sampling flow rates were determined for collecting either a one or three cubic meter sample.

4 RESULTS

4.1 NRL Test Facility Modeling

Initial simulation work was based on typical operating conditions for the NRL Test Facility in Key West. These simulations were designed to investigate the basic modeling requirements for sampling, to assess the fluid flow trajectories for various sample port geometries, and to perform particle injection studies. Throughout the simulations a standard sample flow rate of three cubic meters per hour was used. That rate is indicated in the following figures as the prescribed sample flow rate.

4.1.1 Modeling of Basic Sampling Port Wand Types

Initial CFD simulations were run for four basic sampling port wand configurations:

- A reducing tee directly off the main piping (Figure 12)
- A straight sample pipe inserted radially into the main piping (Figure 13)
- A 90-degree elbow with either a 6-inch or a 2-inch long extension centered on the axis of the main piping (Figure 14)
- A 45-degree elbow centered on the axis of the main piping (Figure 15)

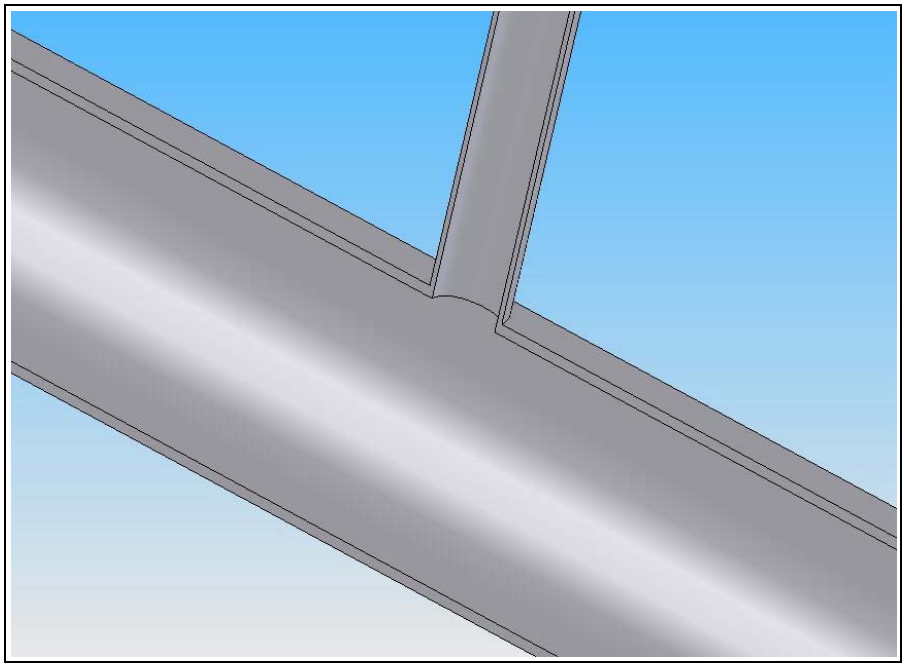

Figure 12. Reducing tee sample port geometry.

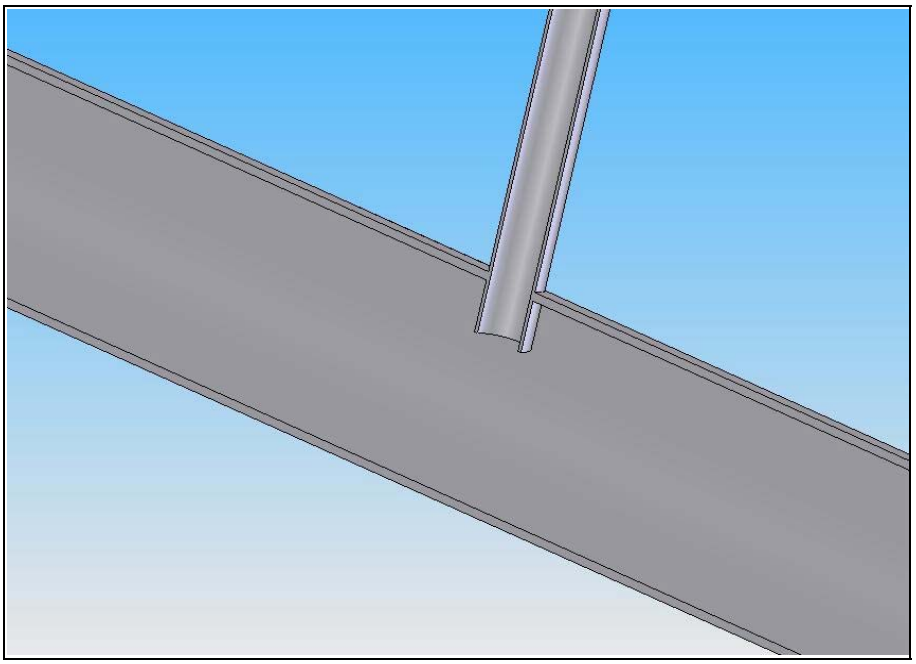

Figure 13. Straight pipe sample port geometry.

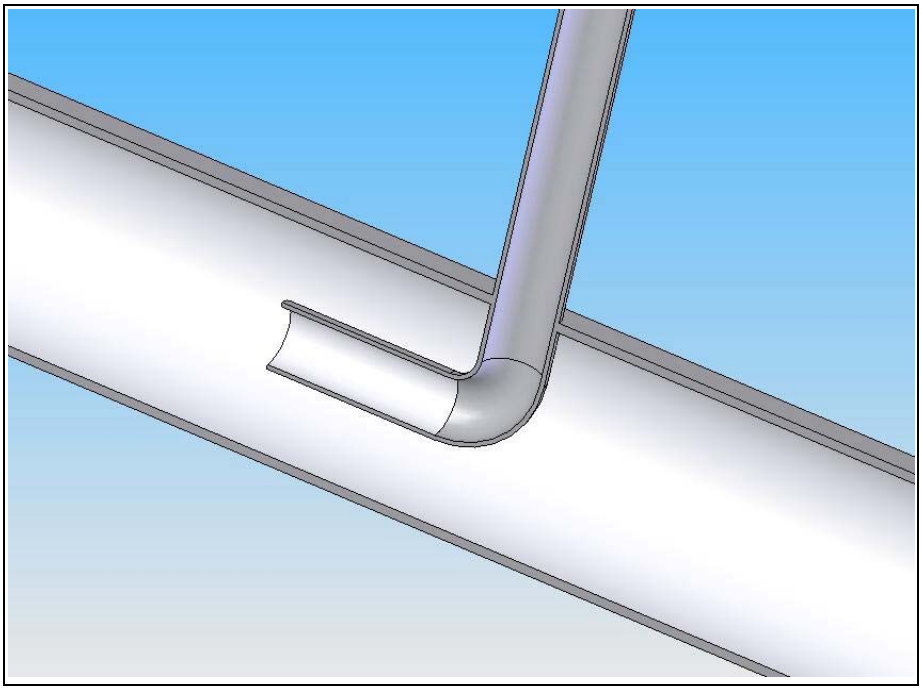

Figure 14. 90-degree elbow with 6-inch extension sample port.

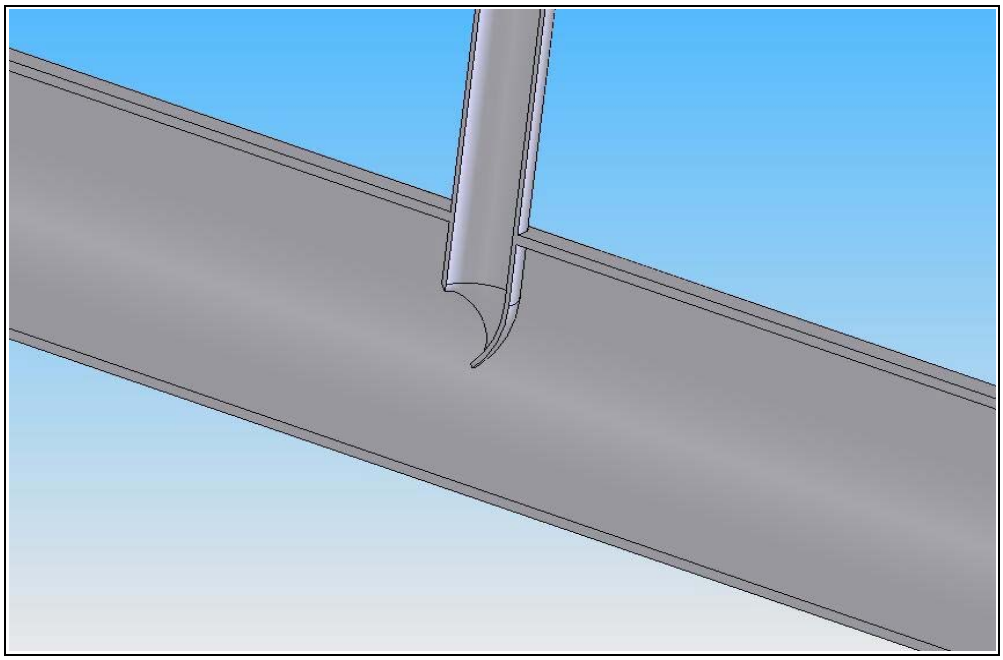

Figure 15. 45-degree elbow sampling port.

4.1.2 Basic Sample Wand Configurations Flow Simulations

The flows for the various wand configurations were analyzed using COSMOSFloWorks® for a section of pipe representative of the supply piping and flow conditions in the BWTTF. The boundary conditions were for typical supply and sampling flow rates, as shown in Figure 16. The supply flow rate was set at 300 cubic meters per hour; the sample flow rate was set at three cubic meters per hour; the outflow boundary condition was set to a constant pressure of one atmosphere. Because the material for piping in the BWTTF is PVC, the wall was assumed to be smooth.

The capability of COSMOSFloWorks® to post-process particle injections was used to study the trajectories of biological organisms introduced into the flow stream. A zooplankton size of 500 microns was modeled, because zooplankton are expected to have the lowest population density and would therefore be more difficult to sample representatively. The biological organisms were modeled as 500-micron spheres having a density equal to that of seawater. These spheres are roughly equivalent to the size of the branchiopod *Artemia* used as a controlled surrogate organism during tests at NRLKW's test facility. The spheres were introduced uniformly into the flow stream on various sections of the entrance boundary to model clear sampling trajectories for all the basic sample wand configurations.

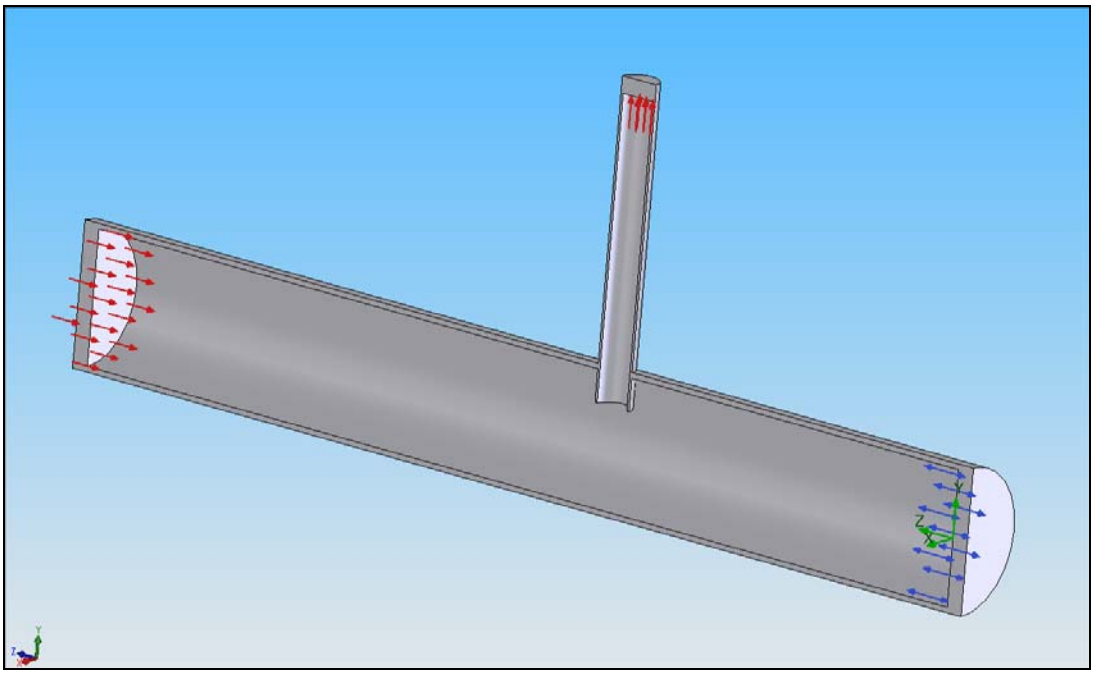

Figure 16. Boundary conditions for BWTTF sample wand simulations.

Figure 17 shows the steady-state velocity profile in the main piping, with no flow from the sample port. The inlet boundary condition is set to fully developed flow. This simulation has no flow at the sample port and is typical of the velocity profile just prior to sampling for all of the sampling port configurations modeled. At these velocities, the entrance length required to establish this flow is approximately 40 diameters. Although fully developed flow is unlikely in shipboard piping, assuming this condition is met in the model allows us to compare the performance of various sampling configurations under the same conditions.

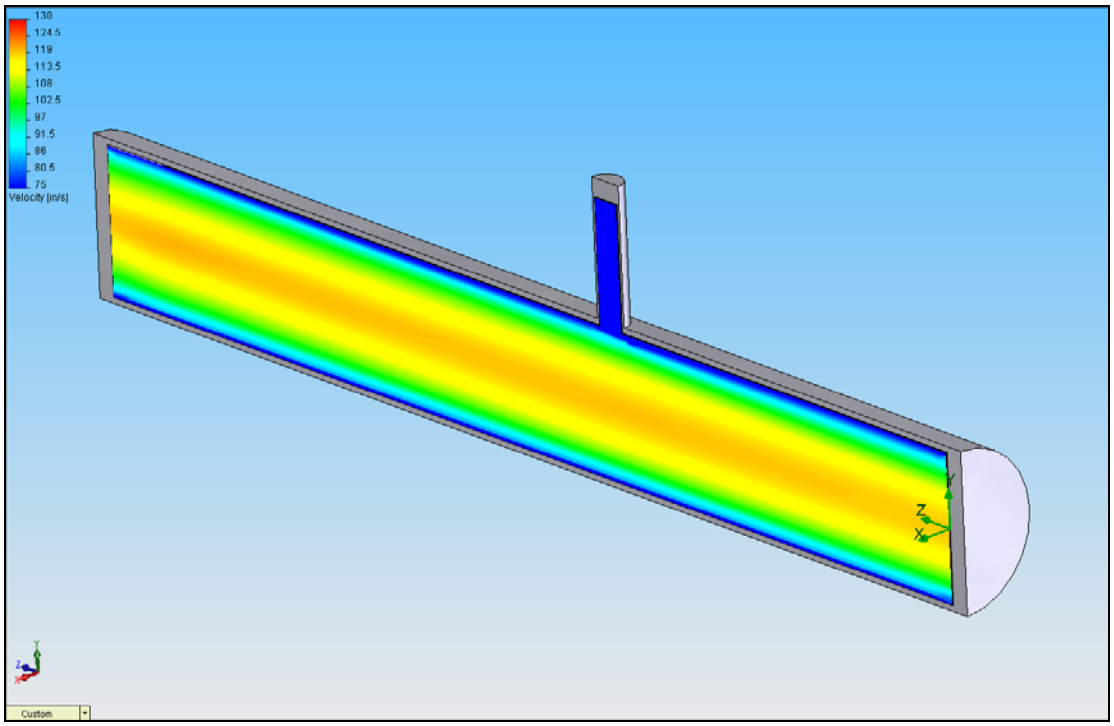

Figure 17. Fully developed centerline velocity contours for BWTTF main piping.

4.1.2.1 Tee Sampling Simulations

Perhaps the simplest configuration for sampling from a pipe is a reduced tee outlet, as shown in Figure 18. This configuration was modeled and analyzed under the conditions listed above. Figure 18 shows the flow trajectories for the exit sample water.

The trajectories clearly show that the sample is taken from very near the wall of the main pipe, essentially in the boundary layer of the main flow. The trajectory lines indicate the flow path of the fluid, where the coloration indicates the variation of velocity along the trajectory. The simulation also shows that there is a large re-circulation zone just inside the entrance of the sample pipe. Figure 19 shows the same results in a 3-dimensional view (note axes).

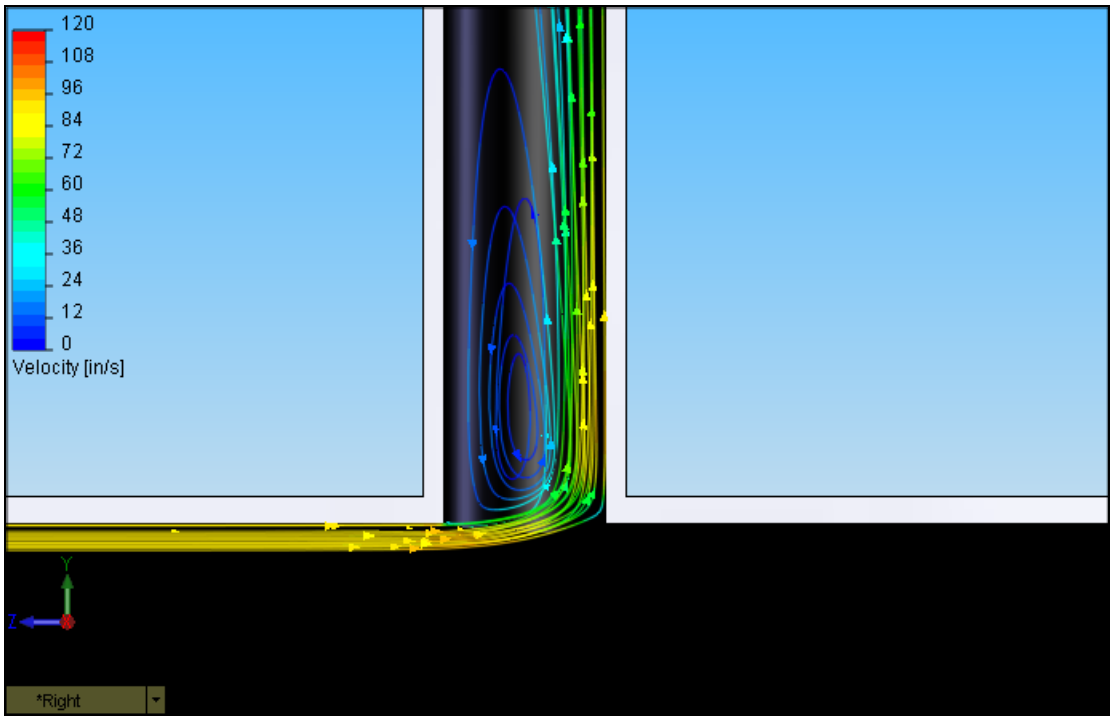

Figure 18. Sample water flow trajectories for tee sampling (front view).

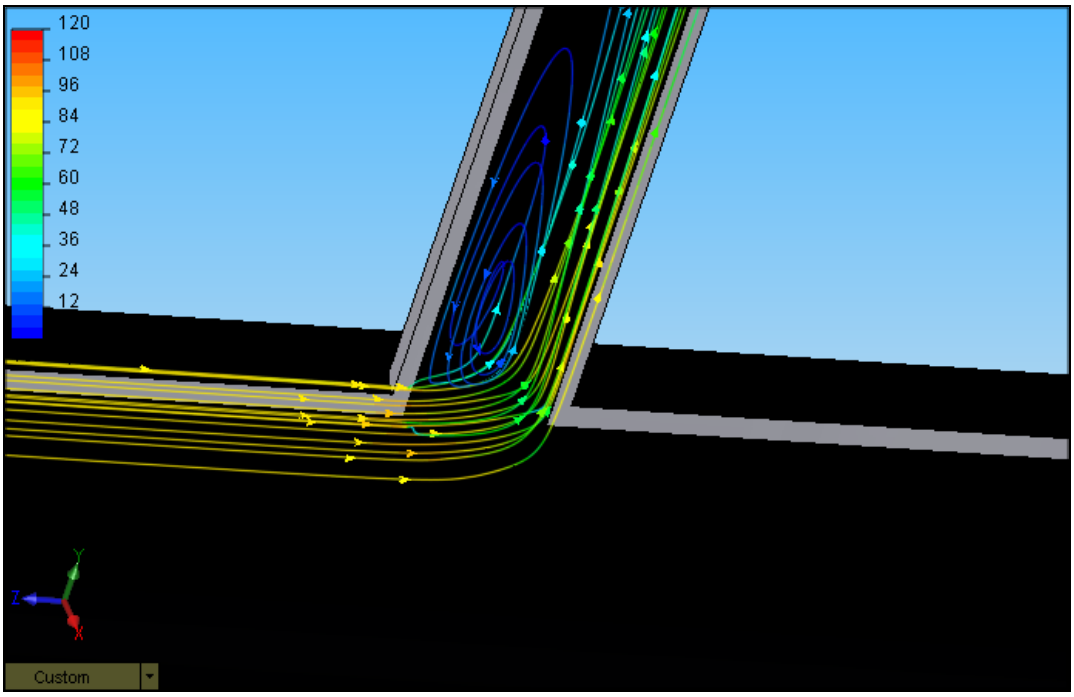

Figure 19. 3-dimensional (isometric) view of sample water flow trajectories (Legend as in Figure 18).

Figure 20 shows the iso-contours of pressure (lines of constant pressure) along the center plane of the sample port. Again the trajectory lines indicate the flow path of the fluid, but here the coloration indicates the variation of pressure along the trajectory. Although there is a sharp increase in pressure at the downstream side of the sample port, the pressure change is at most 1 psi.

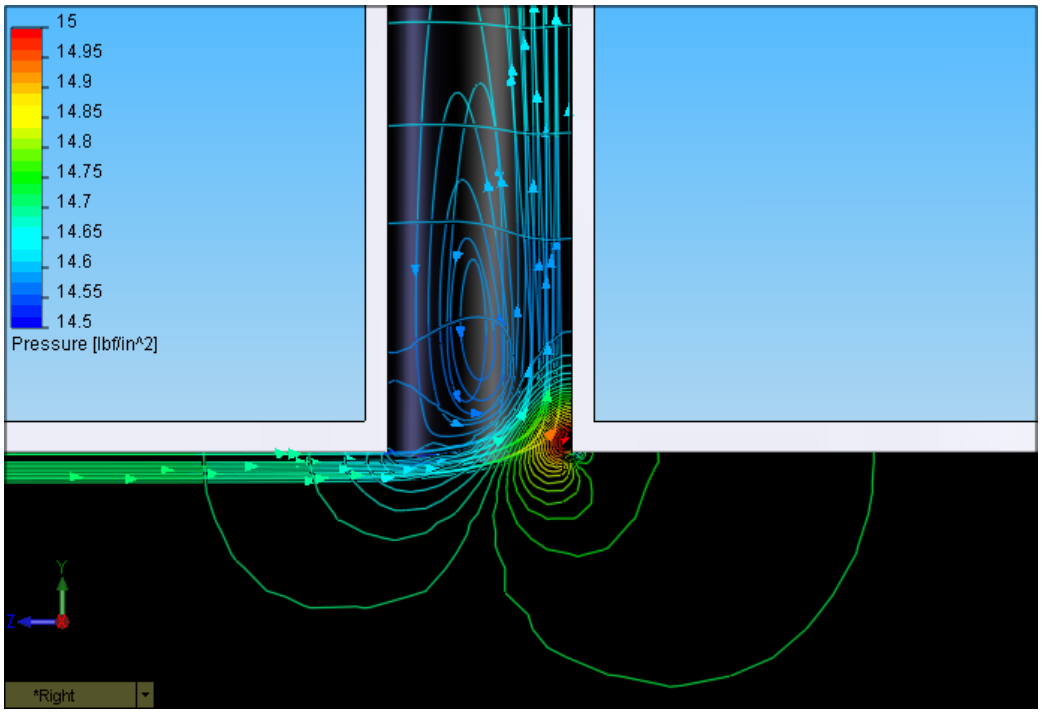

Figure 20. Pressure iso-contours and flow trajectories for tee sampling.

Figure 21 shows the trajectories of particles simulating 500-micron diameter zooplankton introduced into the flow at the entrance. The trajectories and iso-contours are colored as a function of pressure. The particles were only introduced near the outer wall of the pipe, for clarity of presentation. These results clearly show that the biological organisms follow the flow. This result is not unexpected because the biological organisms have the same mass density as water and are small enough to be unaffected by the velocity gradient. One can therefore model the flow for various sample ports and safely assume the biological organisms will follow the flow. These results also indicate that, unlike sampling non-immiscible liquids, oil and water, or particles having significantly different densities than water, sampling will not tend to segregate or separate biological organisms from the sample flow.

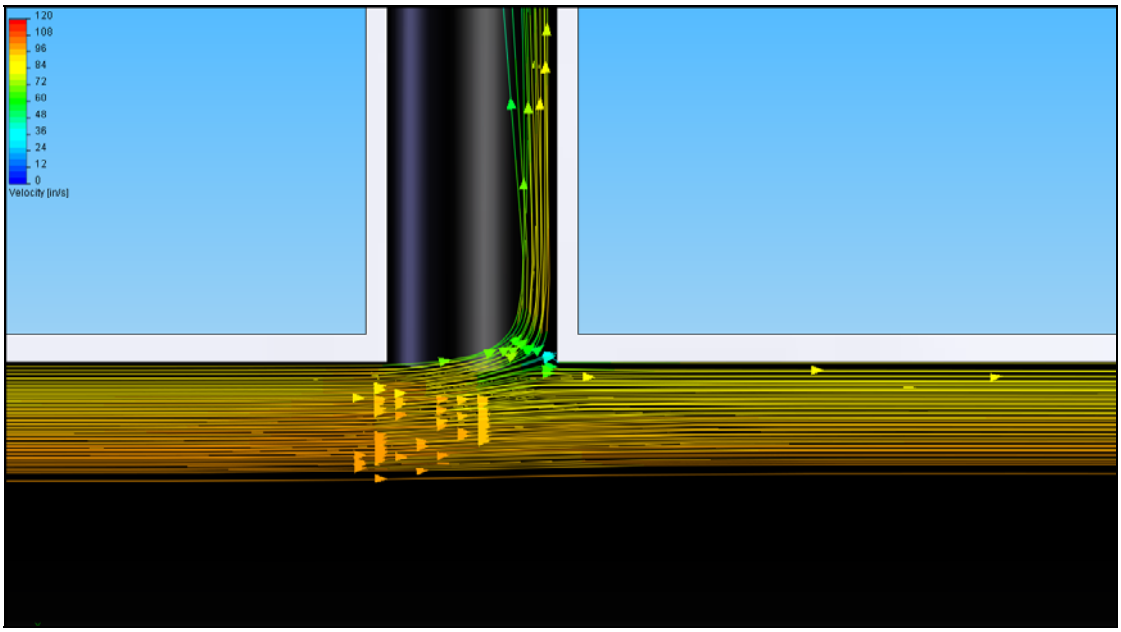

Figure 21. Particle trajectories for tee sampling.

4.1.2.2 Straight Pipe Sampling

The simulations conducted for the tee sampling port were also run for a straight pipe sampler. The coloration of the flow trajectories in Figure 22 indicates velocity. The flow is similar to a tee; however, there is a smaller re-circulation zone, and the sampled flow comes from slightly above the end of the sample pipe. There is also potential for impact of the flow trajectories with the end of the sample pipe, which will likely result in mortality for any organisms following those trajectories.

Figure 23 shows the pressure contours and flow trajectories for this simulation. These are also similar to the tee sample port; however, they also highlight a potential problem with straight-pipe sampling. The pressure in the sample line is below atmospheric pressure, indicating that a pump would be required to draw the sample from the line. The high velocity past the end of the port tends to lower the pressure at the pipe entrance; therefore, unless the pressure difference between the main flow and sample port is high enough, the sampler will require a pump to overcome the pressure differential.

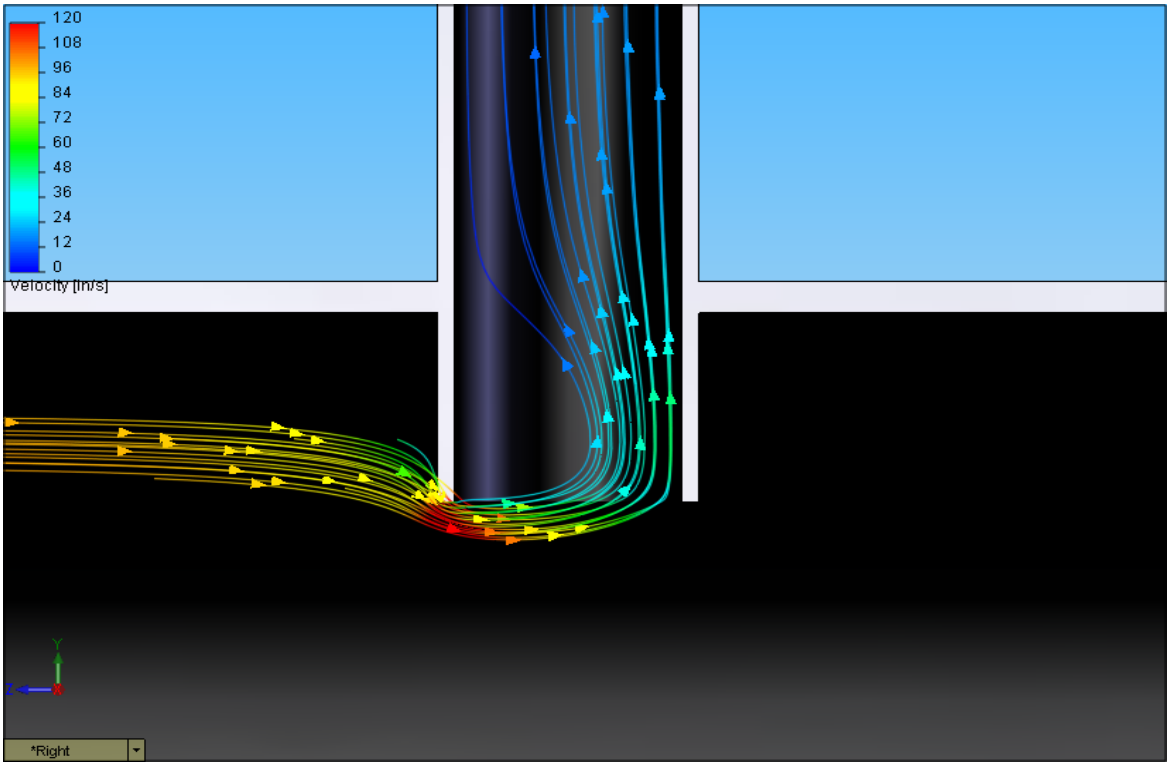

Figure 22. Straight pipe sampler trajectories for a prescribed sample flow rate.

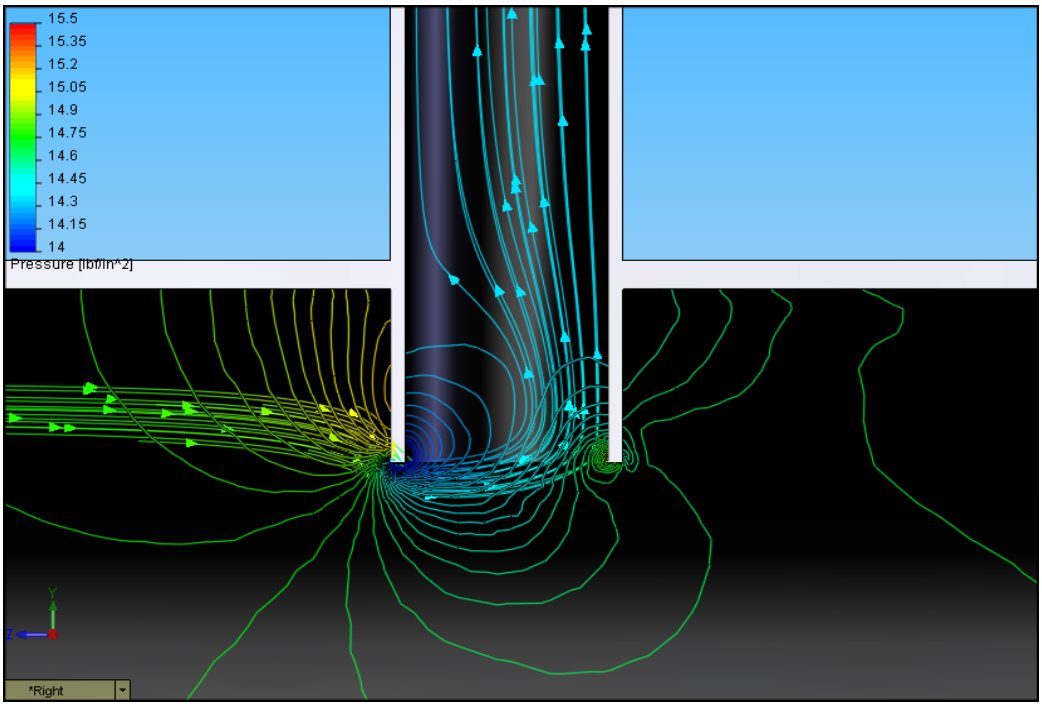

Figure 23. Straight pipe sampler pressure contours and flow trajectories for a prescribed sample flow rate.

This result is demonstrated in Figure 24, which shows the flow trajectories for the same configuration with the sampler boundary condition changed from a prescribed flow rate ($3m^3$/hr) to a pressure equal to one atmosphere. The pressure in the main pipe is a function of the outlet pressure, the rise of the pipe, the length of pipe from the sample location to the exit (including the effect of any valves or fittings), and the velocity in the pipe. Therefore, in situations where sampling is done well below deck by means of long exit piping, there would be no problem sampling by means of a straight tube. However, sampling close to the discharge could easily result in reverse flow in the sample pipe.

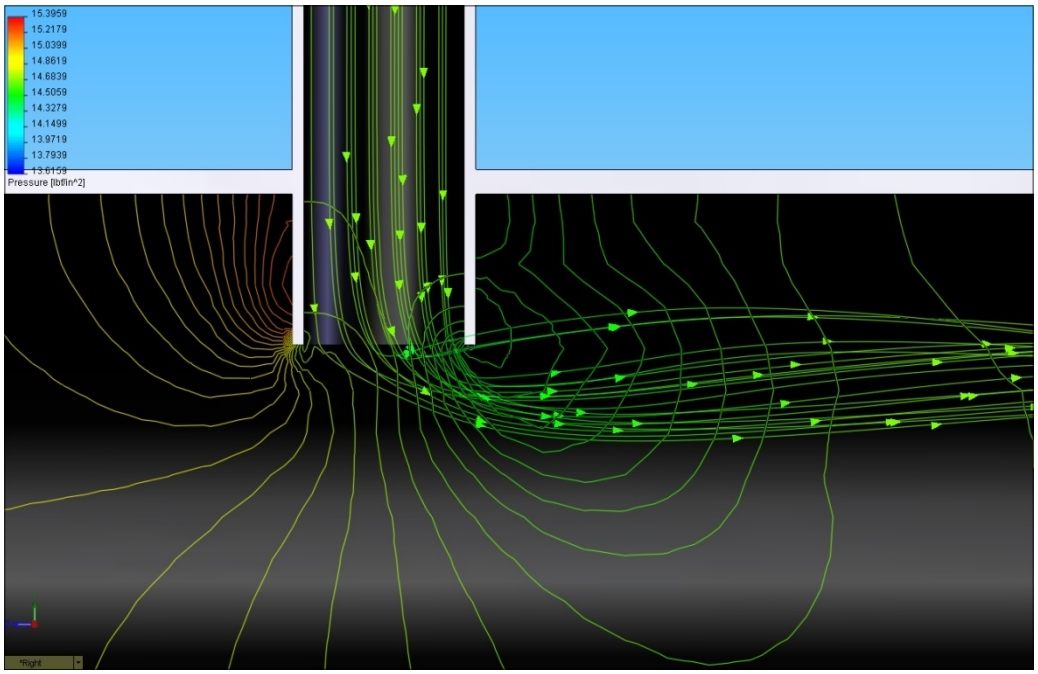

Figure 24. Straight pipe sampler trajectories atmospheric pressure at sample port.

Figure 25 shows the particle trajectories for biological organisms being drawn out of the sampler at the prescribed flow rate ($3m^3$/hr) when the flow and pressure conditions are those presented in Figure 22 and Figure 23 respectively. Again, the particles follow the flow trajectories for the sample flow, further reinforcing the observation that small neutrally buoyant particles will follow the flow.

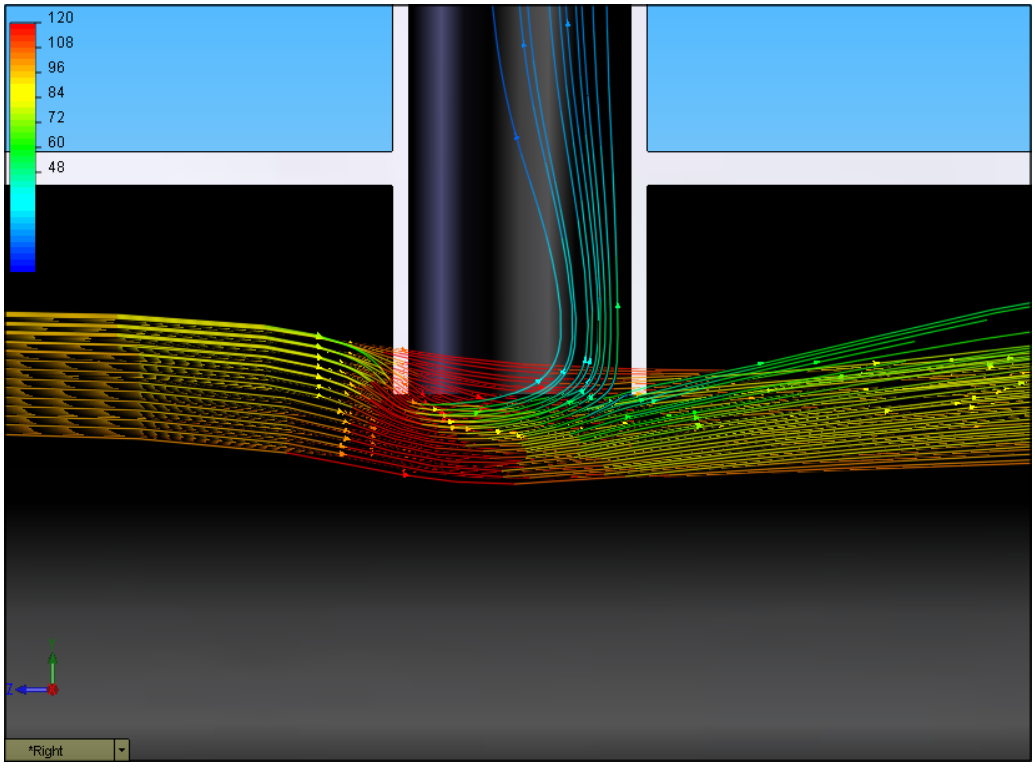

Figure 25. Straight pipe sampler particle trajectories with a prescribed flow rate.

4.1.2.3 Elbow Sampler with 6-Inch Extension

One common form of sampler, previously shown in Figure 14, is a 90-degree elbow turned upstream, with a straight extension oriented into the flow. Figure 26 shows the sampling flow trajectories and velocity contours for this sampler. The elbow system shown has a 6-inch straight extension. The flow trajectories inside the sample pipe are particularly well behaved. There is a smooth transition from the main flow into the sampler, and there are no back-flow eddies in the sample pipe. The sample is taken primarily from the centerline flow in the main pipe, from a diameter that matches the volumetric flow rate of the sample taken. This diameter is identical to the isokinetic diameter (previously discussed in Section 3.3) used in many pipe-sampling systems, where separation of dissimilar flow constituents might occur.

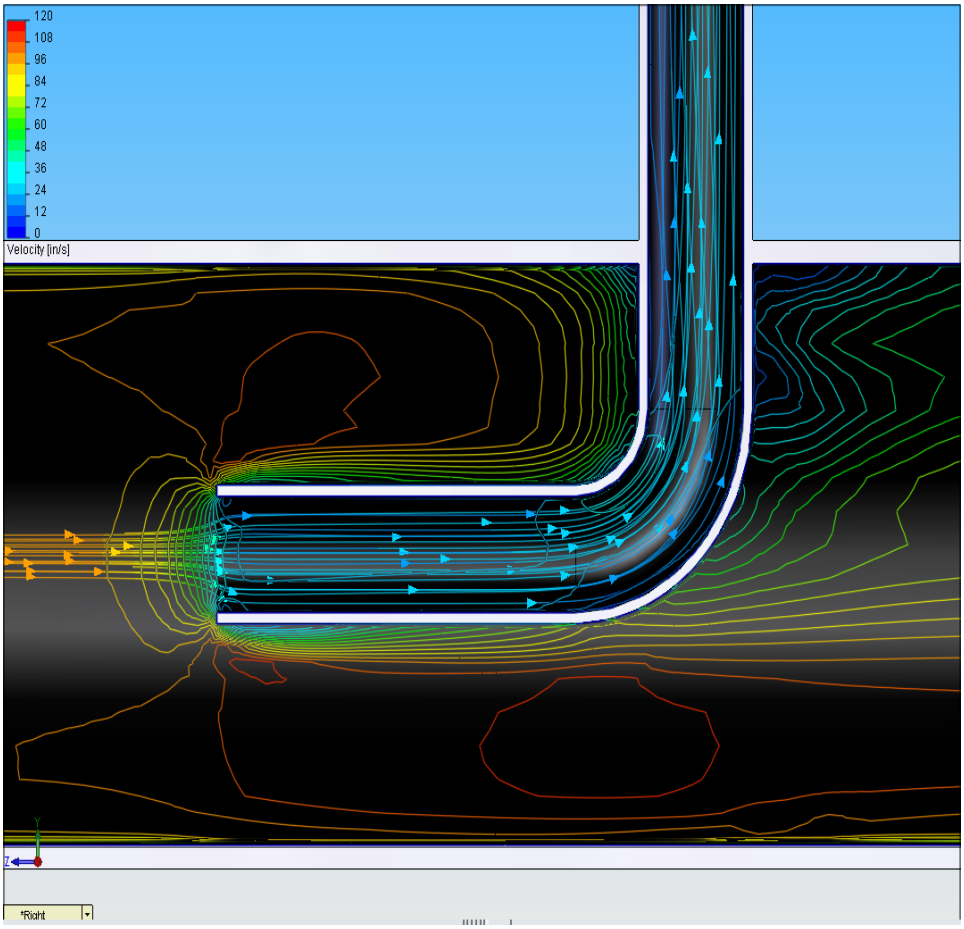

Figure 26. Velocity contours / flow trajectories for elbow sampler with 6-inch extension.

Figure 27 is a plot of the same flow trajectories showing iso-contours of pressure for the same simulation. As would be expected, the smooth velocity transitions imply a similar smooth transition in pressure from main pipe pressure of slightly over 14.7 psi to slightly over 15.3 psi in the sample pipe.

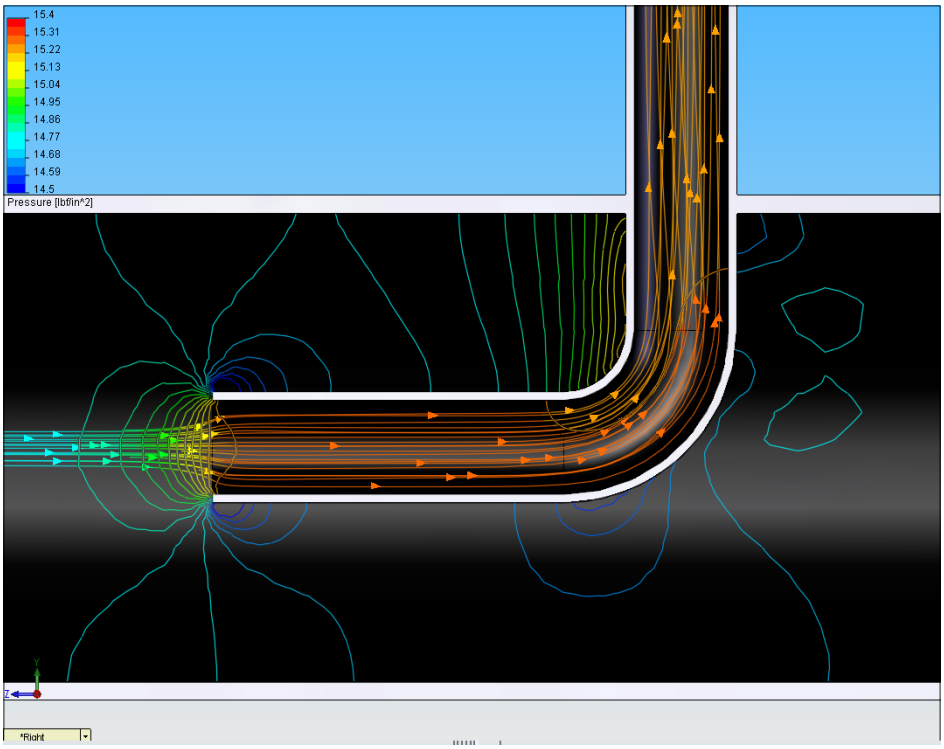

Figure 27. Pressure contours/flow trajectories for elbow sampler with 6-inch extension.

Particle trajectories for this simulation are shown in Figure 28, where the trajectory coloration indicates velocity. As expected, these trajectories follow the flow contours presented above. Transition from the main flow stream to the sample flow stream is a gradual transition, with the particles flowing smoothly around the sample elbow.

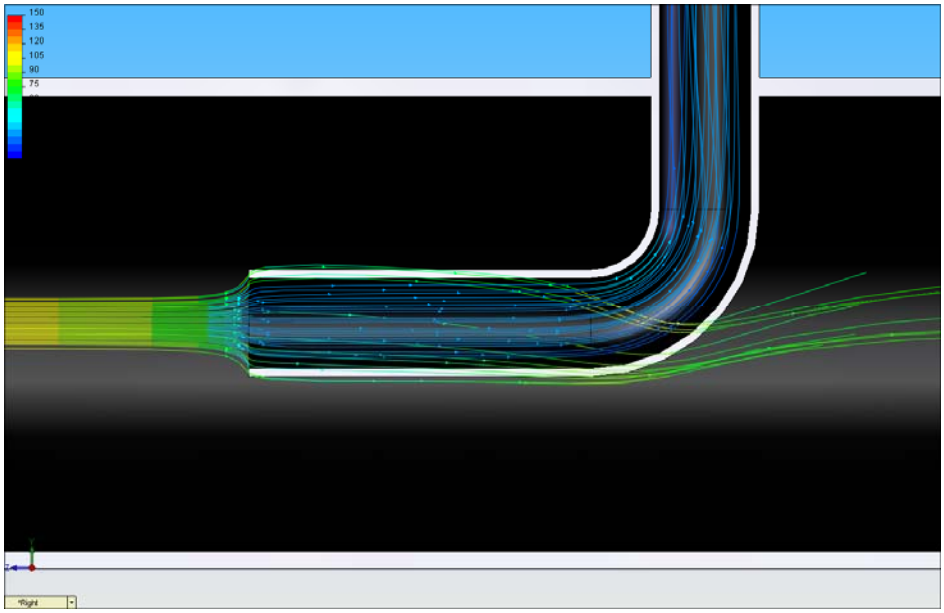

Figure 28. Trajectories of injected particles for an elbow sampler with a 6-inch extension.

4.1.2.4 Elbow Sampler with 2-Inch Extension

The flow patterns for the elbow with a 6-inch extension show that the transition from the main flow to a nearly uniform velocity in the sampler occurs within a diameter or so of the sample point. This result implies that little if anything is gained from having a long upstream extension. Figure 29 and Figure 30 demonstrate the same conclusion holds for a sampler with the extension reduced to two inches. Figure 29 presents flow trajectories and velocity contours for the 2-inch extension, while Figure 30 presents the results for pressure contours. The character of the sample flow is identical to that of the 6-inch extension. The 2-inch extension would be preferred because of easier installation.

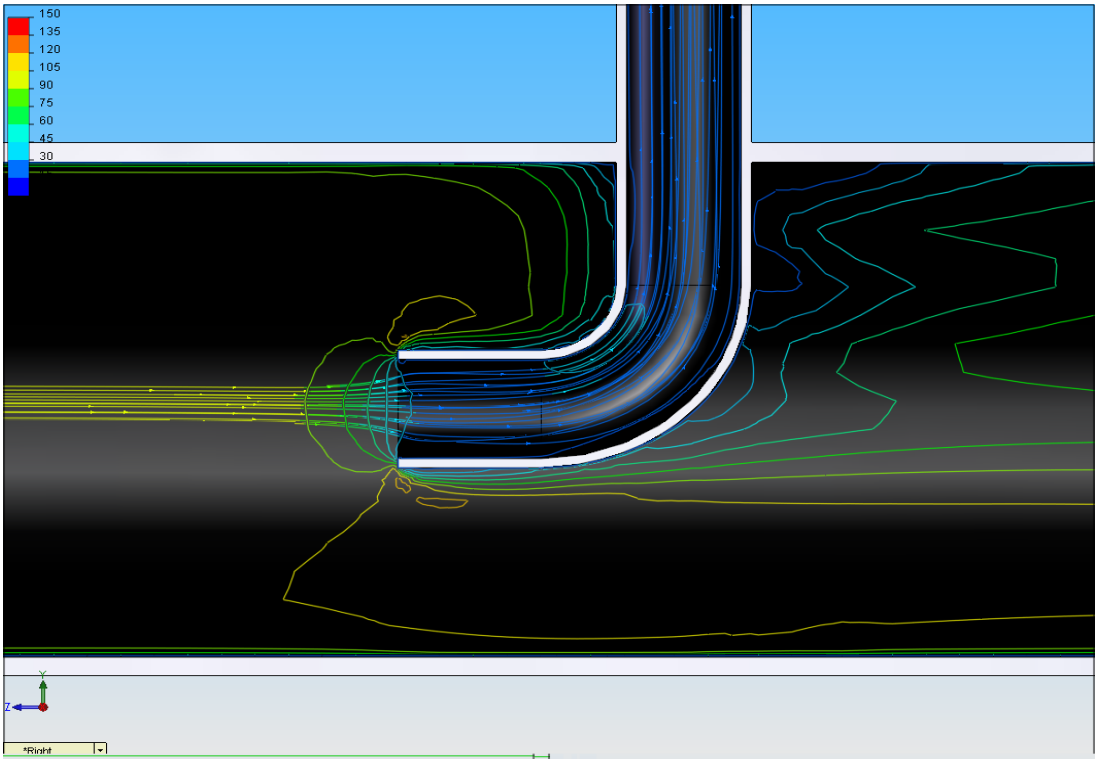

Figure 29. Flow trajectories and velocity contours for elbow with 2-inch extension.

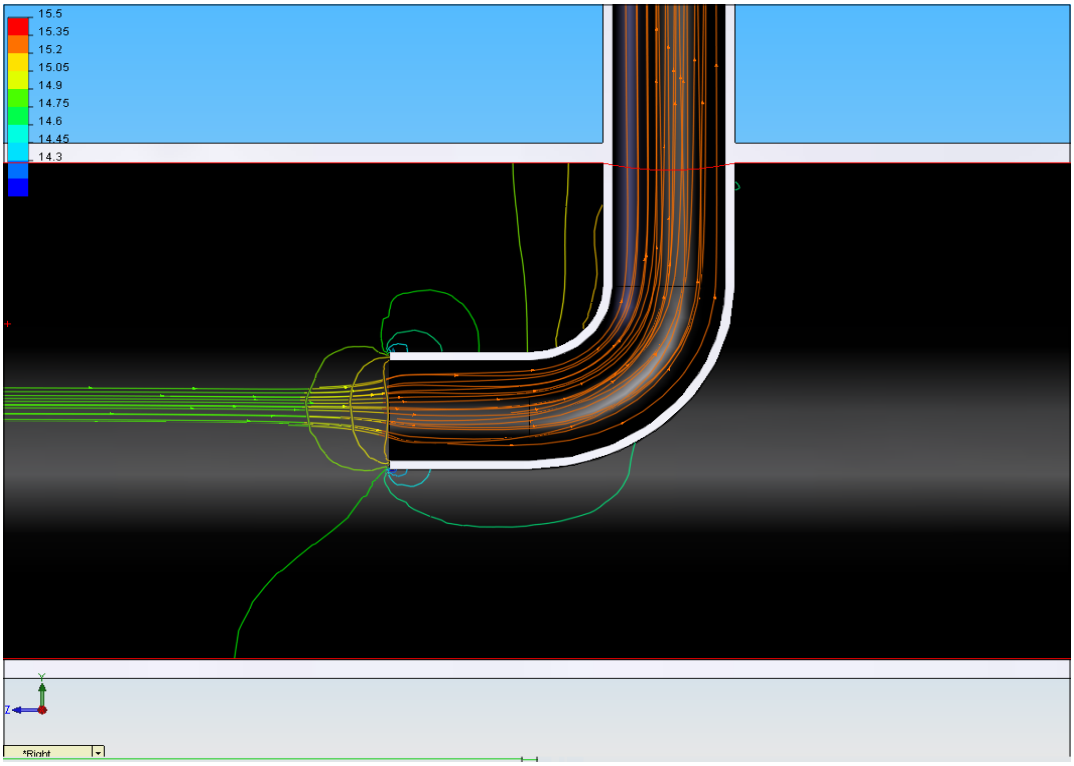

Figure 30. Flow trajectories and pressure contours for elbow with 2-inch extension.

4.1.2.5 45-Degree Cut Elbow Sampling

One additional sampler geometry was analyzed—an elbow cut at 45 degrees. The flow trajectories and velocity contours for this configuration are shown in Figure 31. This configuration samples primarily from the top of the 45-degree cut and has a significant re-circulation zone, similar to the tee sampler. The flow trajectories show that particles would be swept along the backside of the sample tube, increasing the likelihood of impact with the sampler walls. Figure 32 shows the same flow trajectories as a function of velocity in a 3-dimensional view. Figure 33 presents the pressure contours and flow trajectories for the cut elbow.

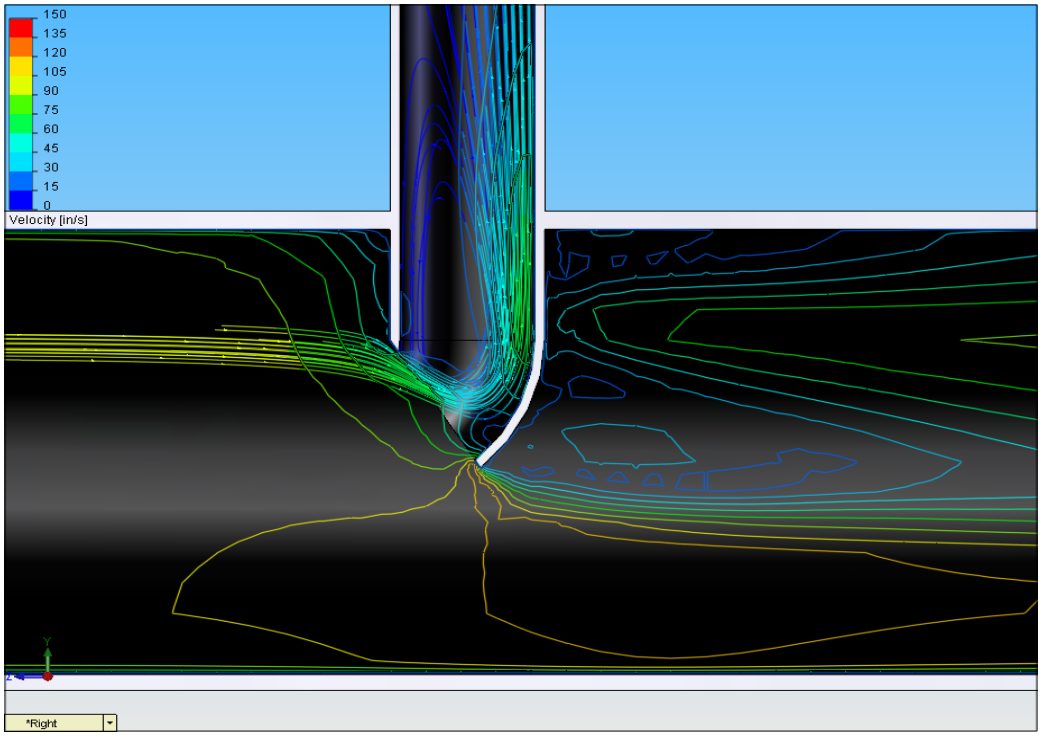

Figure 31. Flow trajectories and velocity contours for 45-degree cut elbow.

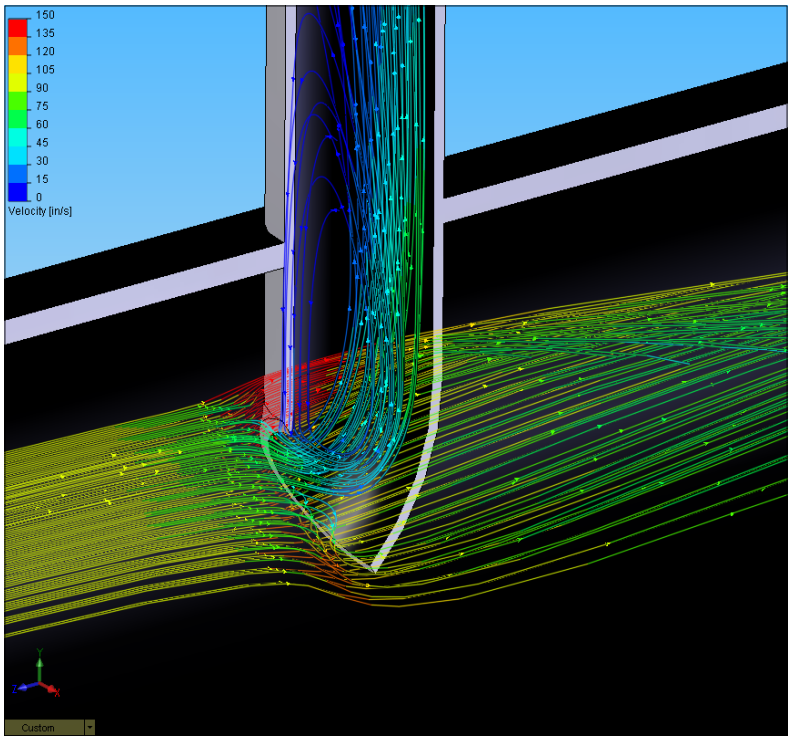

Figure 32. Flow trajectories for 45-degree cut elbow.

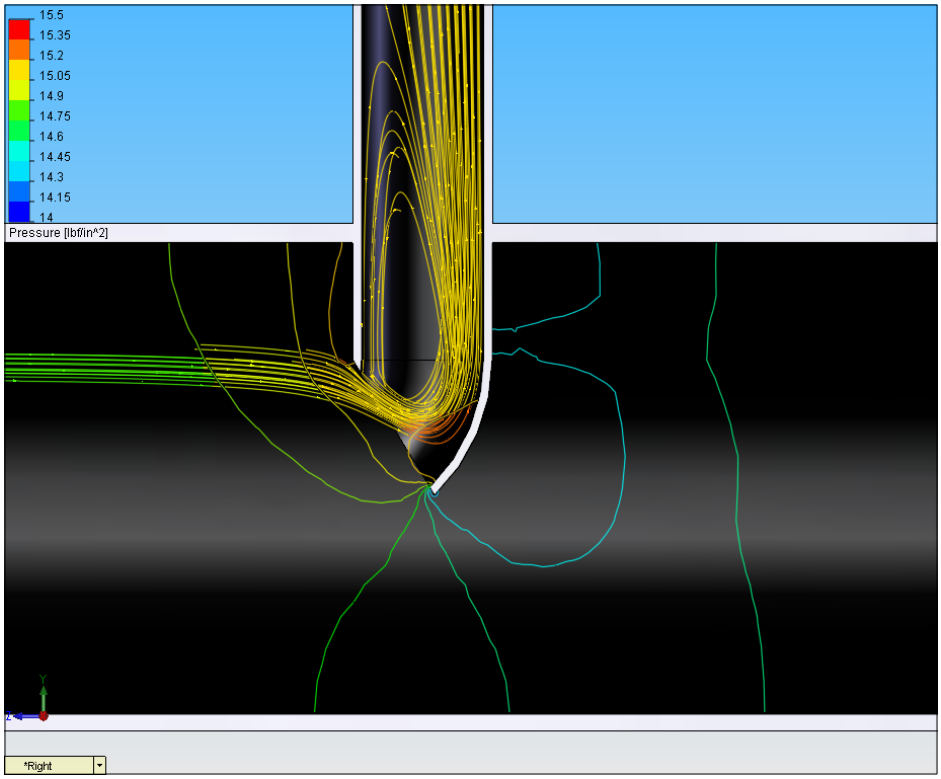

Figure 33. Pressure contours and flow trajectories for 45-degree cut elbow.

The sample port investigations show that the design and position of the port can have a significant effect on the location from which the sample is drawn within the flow stream, on the trajectory of the particles within the flow, and on the pressure differentials that must be overcome by the sampling system. The sampling port design for the 2-inch and 6-inch elbow samplers were the least likely to have re-circulation or particle impacts; showed a smooth transition of velocity and pressure from the main pipe to the sampling pipe; and will have minimal effect on biological organisms within the flow stream. The 2-inch sampler has the added benefit of reduced size for ease of installation.

4.2 Injection System Modeling

At the BWTTF, ambient seawater is used as the source for ballast water testing. To achieve the organism densities required by the ETV test protocols, and to provide standard test organisms to all test runs, zooplankton and phytoplankton are injected into the ballast water flow stream. Various methods for biological organism injection were evaluated under efforts described by Lemieux et al. (2005). On the basis of this previous work, the BWWTF incorporated a pressure-based injection system to generate the requisite organism densities in the ballast flow.

CFD models were developed for the BWTTF main piping, including the injection piping area, to investigate the distribution of injected biological organisms at the sampling location. An isometric layout of the main piping model is shown in Figure 34. The main piping consists of approximately 10-foot lengths of 8-inch PVC, with the injection and sampling ports 4 feet from the inlet and outlet.

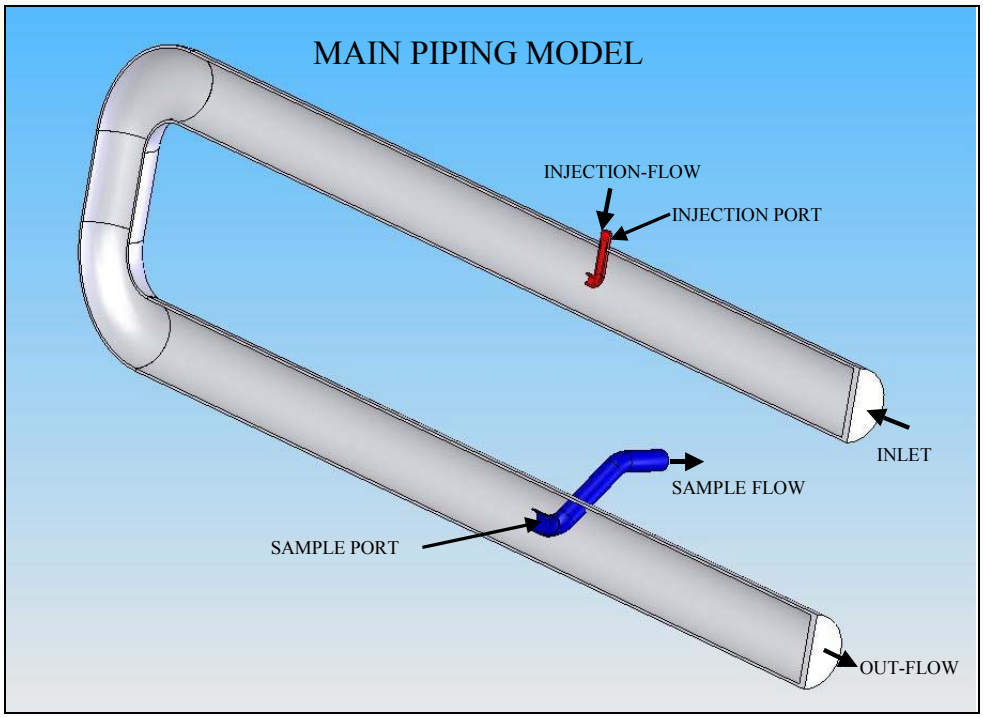

Figure 34. Main piping injection section model for the BWTTF.

Simulations were run to investigate the basic flow profiles in the main piping and the mixing of a fluid introduced at the injection port. To perform these latter simulations, the capability of COSMOSFloWorks® to model multiple species of fluids was employed. Both the main and injected flows were modeled as seawater, but they were given distinct definitions—Water 1 and Water 2—so that their individual concentrations could be monitored throughout the system. Because it has been established that biological organisms will follow the flow, the concentration of the injected water (Water 2) can be used to calculate the biological concentrations at any location.

Figure 35 shows, as an orthogonal view, the velocity contours along the vertical centerline plane of the main piping, with a fully developed flow field at the inlet and no secondary injection. Although the velocity is fairly uniform across the section before the first elbow, the transition through the elbows sets up a noticeable non-uniformity, with a high velocity on the bottom of the main pipe, that does not equilibrate before the location of the sample port.

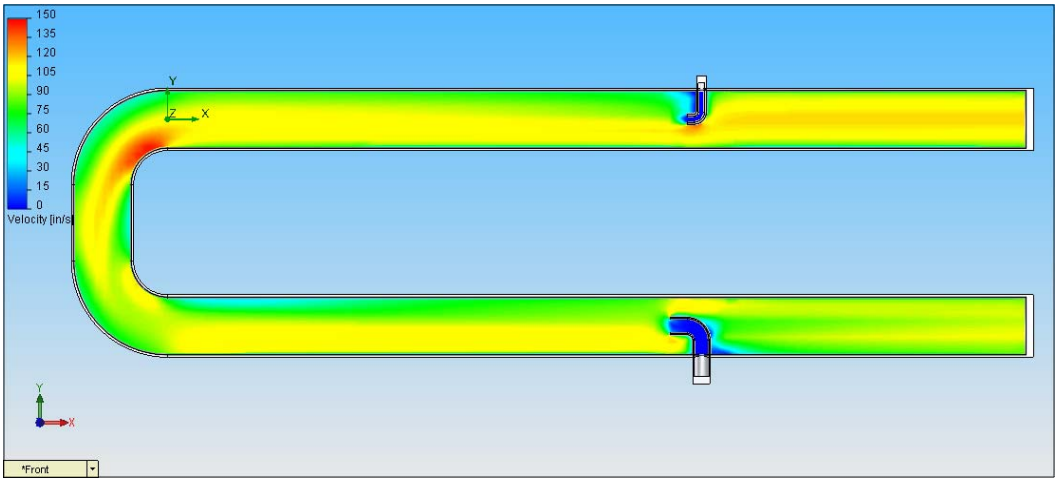

Figure 35. Velocity contours for main piping.

One would expect from this result exactly the non-uniformity in the distribution of injected water that is shown in Figure 36, which is a plot of the injected water fraction on the centerline plane of the main piping. The injected water fraction is the ratio of injected water volume to main inlet water volume at any given location. Thus, the injected water fraction at the main inlet is 0, and at the injection port is 1. The injected water fraction is plotted over the range of 0 to 0.003, in order to highlight the variation in the mixing. Any fraction above 0.003 is shown in the figure in deep red. The concentration for a uniform mixture of primary and injected water would be the volume fraction 0.00056 and would show as a light blue in the figure.

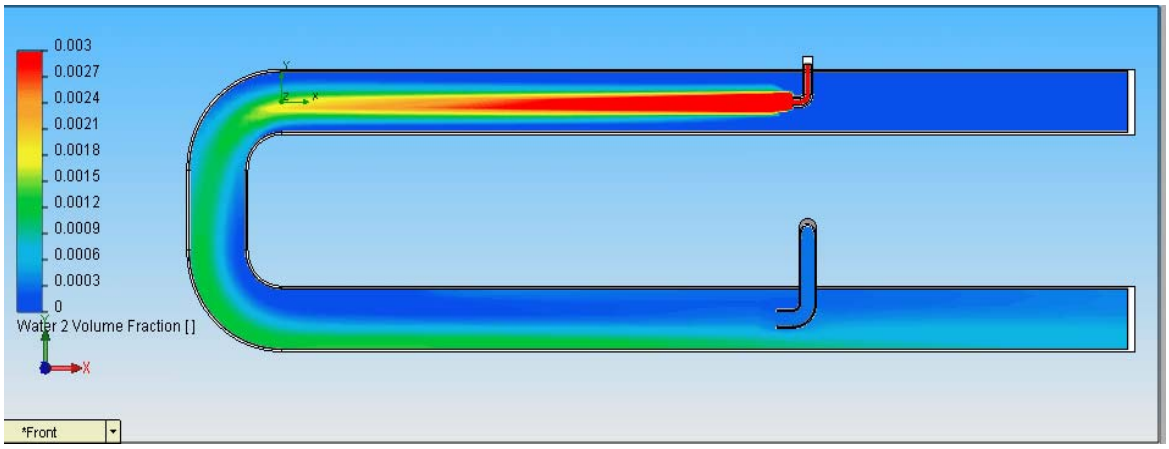

Figure 36. Concentration of injected sample water in main piping.

The injected water does not have time to mix uniformly before the elbows, and a significant fraction of the injected water is swept outside on the return elbow, resulting in a non-uniform distribution concentrated along the bottom of the return pipe.

Using the capability of COSMOSFloWorks® to calculate integrated quantities on specified boundaries, the total volume fraction of injected water can be determined for the sample port and main outlet. These values are presented in Table 5. The volume fraction of injected water is only 0.0003 at the sample port outlet, which represents only 54 percent of what the fully mixed volume fraction should be. Therefore, this configuration would only sample 54 percent of the biological organisms that would be present at the sample port if the flows were fully mixed.

Table 5. Injected water concentration at the sample port.

Parameter	Value	% Fully Mix
Injected Water Fully Mixed Volume Fraction	0.00056	
Injected Water Fraction at Sample Port	0.00030	54%
Injected Water Fraction at Outlet	0.00056	100.0%

This simulation assumes that the inlet boundary is fully developed, and that there is no swirl of the flow around the centerline of the pipe. However, in most real-world flows, the effect of pumps is to induce considerable swirl in the flow that is generally slow to dissipate. At the BWTTF, ballast flow enters the modeled section by way of two pumps, with flow entering through a pair of fittings orthogonal to the modeled flow. To better represent these flow conditions, Figure 37 shows the flow trajectories as a function of velocity for the case of a 10-radian per second swirl (a reasonable swirl value for the BWTTF piping) at the input boundary. The braided appearance of the trajectories up to the return elbows indicates that this input condition would lead to far greater mixing of the main and injected flows.

Figure 38 is a plot of the volume fraction of injected water on the centerline plane of the pipe, clearly showing improved mixing with the swirl included. Compared to the mixing shown in Figure 36, the swirled mixing is far more uniform at the sample port. This level of uniformity is confirmed by the surface integral calculations for volume fraction presented in Table 6. With swirl included in the model, the sample volume fraction is now 91 percent of the fully mixed concentration.

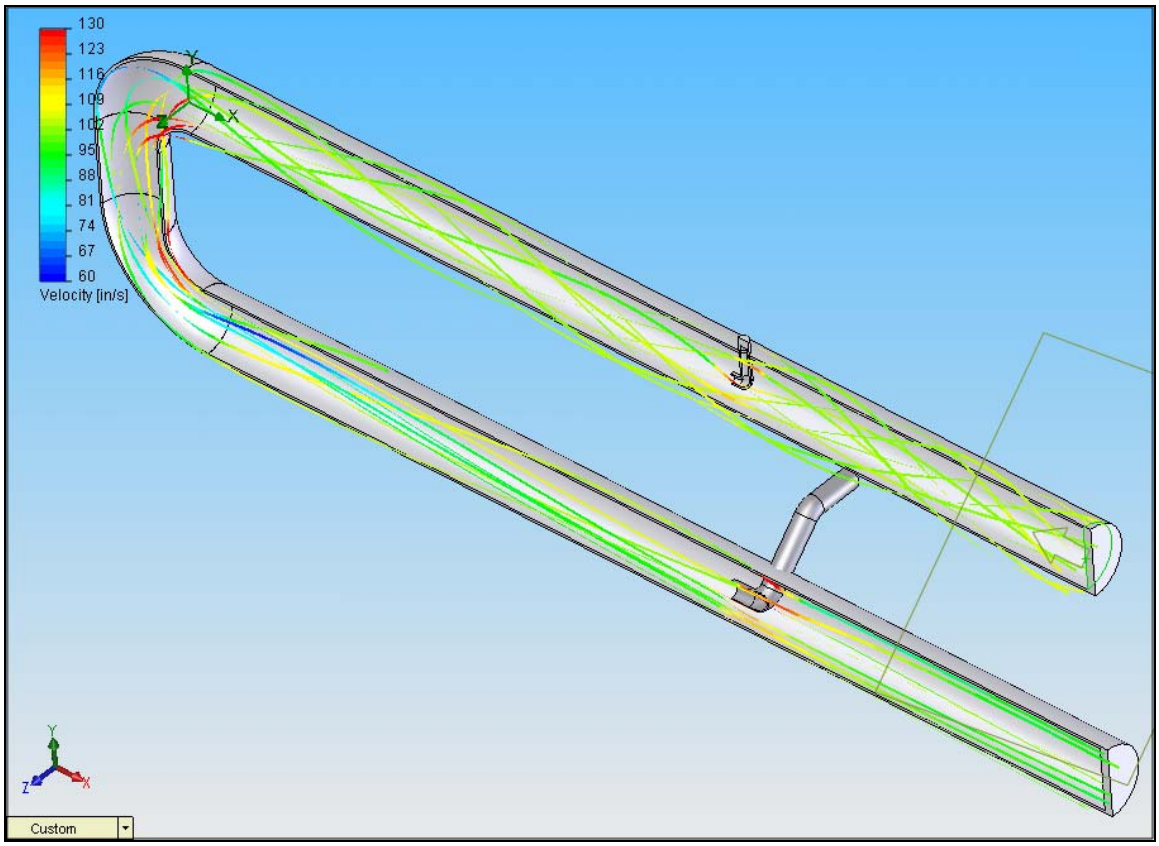

Figure 37. Flow trajectories with swirl from input pump.

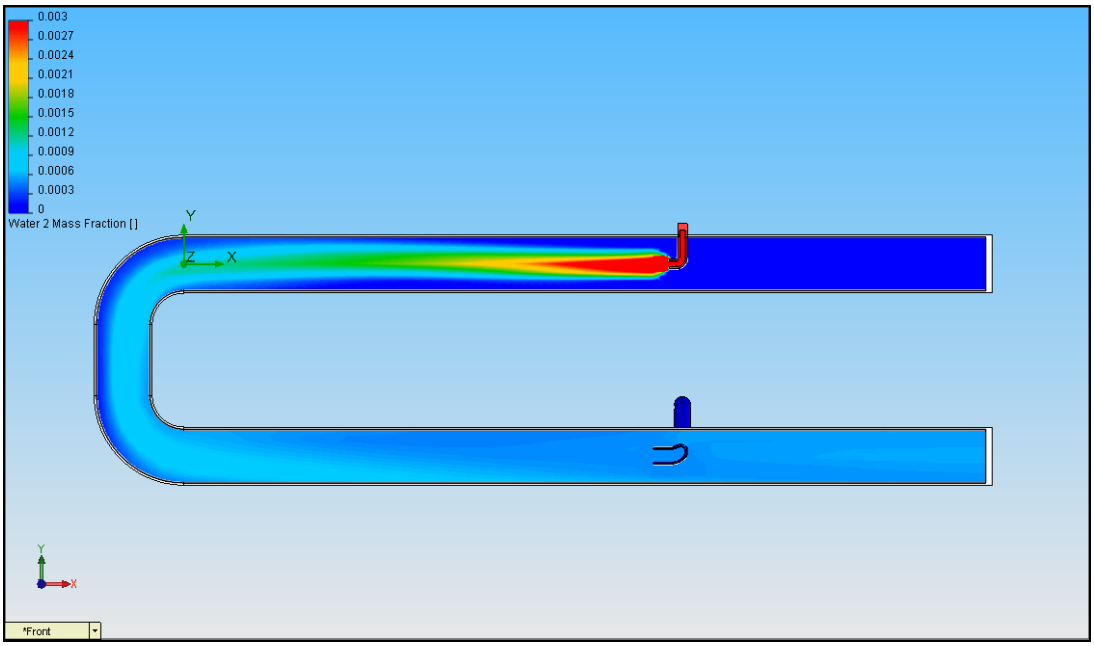

Figure 38. Concentration of injected water for swirled input.

Table 6. Injected water concentrations at sample port with swirled input.

Parameter	Value	% Fully Mixed
Injected Water Uniform Volume Fraction	0.00056	
Injected Water Fraction at Sample Port	0.00051	91%
Injected Water Fraction at Outlet	0.0056	100%

4.3 Multi-Port Sampling

Some protocols for sampling ballast water require that independent samples (often three are specified) be taken simultaneously at the same location. This requirement is open to interpretation as to what is meant by 'same location', but the most logical interpretation would seem to be 'the same cross sectional location along the ballast water discharge pipe'.

One approach to implementing this interpretation is shown in Figure 39, where three elbow sampling ports are located 120 degrees apart, an equal radial distance from the centerline of the pipe, and at the same cross section. Implementing such a system requires additional flanges and piping, and might be difficult to locate on some shipboard installations. However, with regard to meeting the simultaneous sampling requirement, the only fluid dynamic question is: Will these now be independent and not interact hydrodynamically?

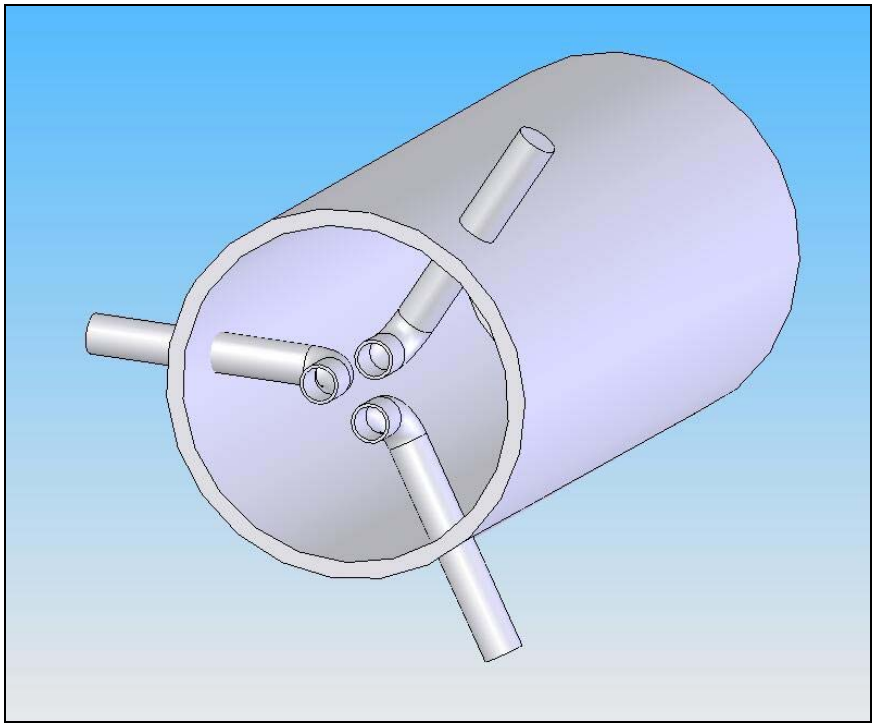

Figure 39. Three-port sampling configuration.

Figure 40 shows flow trajectories plotted as a function of velocity for the sampling configuration described above. Clearly, the flow trajectories into the three sample ports do not interact and are thus independent. Furthermore, the flow through the sample wands is identical to those for a single port located at the center. For a fully developed and mixed flow, this approach would meet all of the sampling requirements listed. However, it should be noted that for the three ports to truly be at the 'same location' in a fluid-dynamic sense, the sampling must occur in a long straight pipe section (with the entrance length calculated with Equation 3) to ensure that the pipe flow is fully developed. Given these conditions, this type of sampling approach (the three-port sampler) can provide three independent samples.

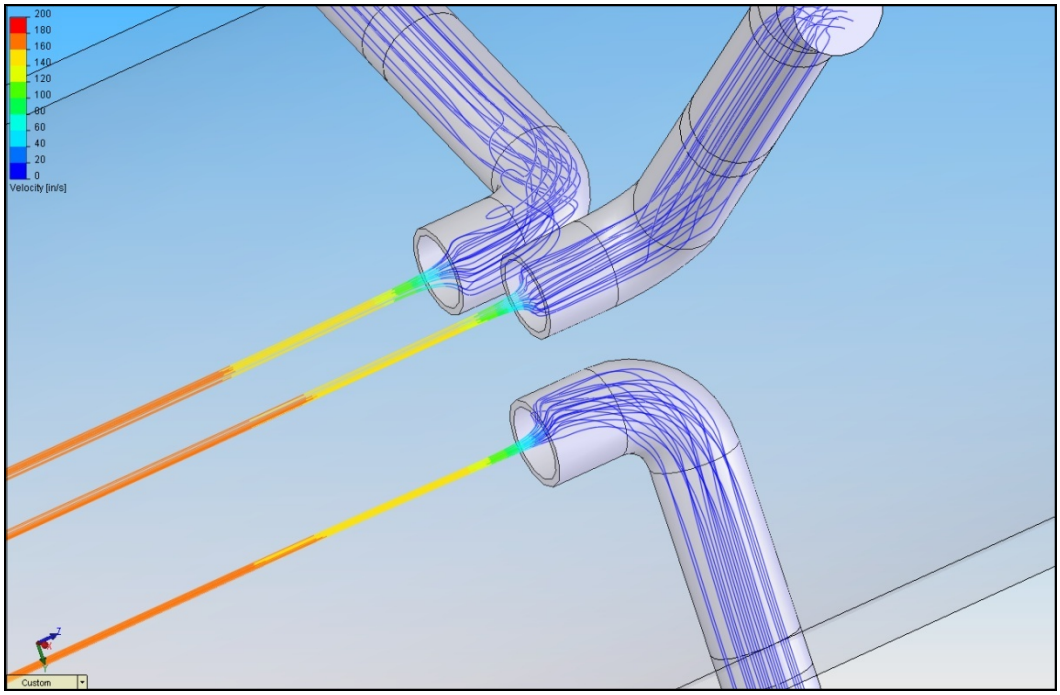

Figure 40. Flow trajectories for 3-port sampler.

5 DISCUSSION

Figure 41 shows the overboard ballast water piping for the NANUQ, a 3554-ton, 301-ft Arctic supply ship commissioned on May 1, 2007. The ballast system is composed of 15 separate ballast tanks piped to a single 1400-gpm pump. For this exercise, it was assumed that the port and starboard ballast tanks were being discharged simultaneously, and that a total sample volume of three cubic meters would be collected.

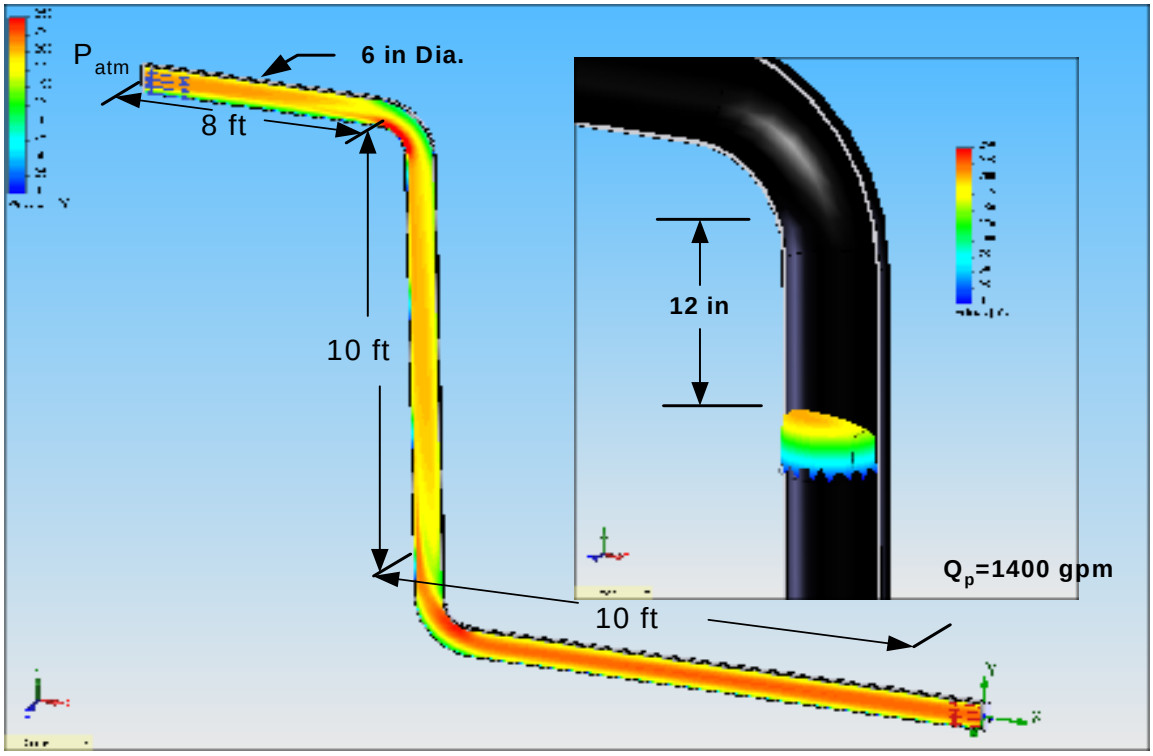

Figure 41. Ballast water overboard piping and basic velocity profiles.

The total volume for the port- and starboard-bow ballast tanks is 300 cubic meters; therefore, the time required emptying the tanks is:

$$T_B = \frac{V_B}{Q_B} \qquad T_B = 57\,\text{min}$$

where:

pump flow-rate is: $Q_B = 1400\,\frac{\text{gal}}{\text{min}}$ or $5.3\,\frac{\text{m}^3}{\text{min}}$

ballast volume is: $V_B = 300\,\text{m}^3$

For a sample volume of three cubic meters, the sample flow rate is calculated as:

$$Q_{Sp} = \frac{V_{Sp}}{T_B} \qquad Q_{Sp} = 14\,\frac{\text{gal}}{\text{min}}$$

where the sample volume is: $V_{Sp} = 3\,\text{m}^3$

From these results, we can make a preliminary calculation of the required sample port diameter, based on the isokinetic port diameter, where:

$$D_{iso} = D_B \sqrt{\frac{Q_{Sp}}{Q_B}} \qquad D_{iso} = 0.6 \text{ in}$$

and the ballast water-pipe diameter is: $D_B = 6 \text{ in}$

Given that the sample port should be between 1.5 and 2 times the isokinetic diameter, an initial working sample port diameter was calculated as two times the isokinetic diameter:

$$2 \cdot D_{iso} = 1.2 \text{in}$$

However, for real-world applications, the actual sample port should be a standard pipe size. For example, a standard 1-inch Schedule 40 pipe such as is used in the test facility piping has an inside diameter of 1.049 inches. This diameter would yield an isokinetic diameter ratio of:

$$\frac{D_{1NP}}{D_{iso}} = 1.748$$

where: $D_{1NP} = 1.049 \text{ in}$

Based on the NANUQ's overboard piping configuration, the best location for a sample port is at the top of the 10-foot vertical risers, just before the elbow. Because there is an elbow in the main pipe, the sample port can be introduced through a flange on the elbow, thereby negating the need for an elbow in the sampler itself. This configuration is shown in Figure 42. The entrance to the sample wand is located 12 inches (2 pipe diameters) away from the elbow to minimize the affects of the elbow on flow distribution near the port.

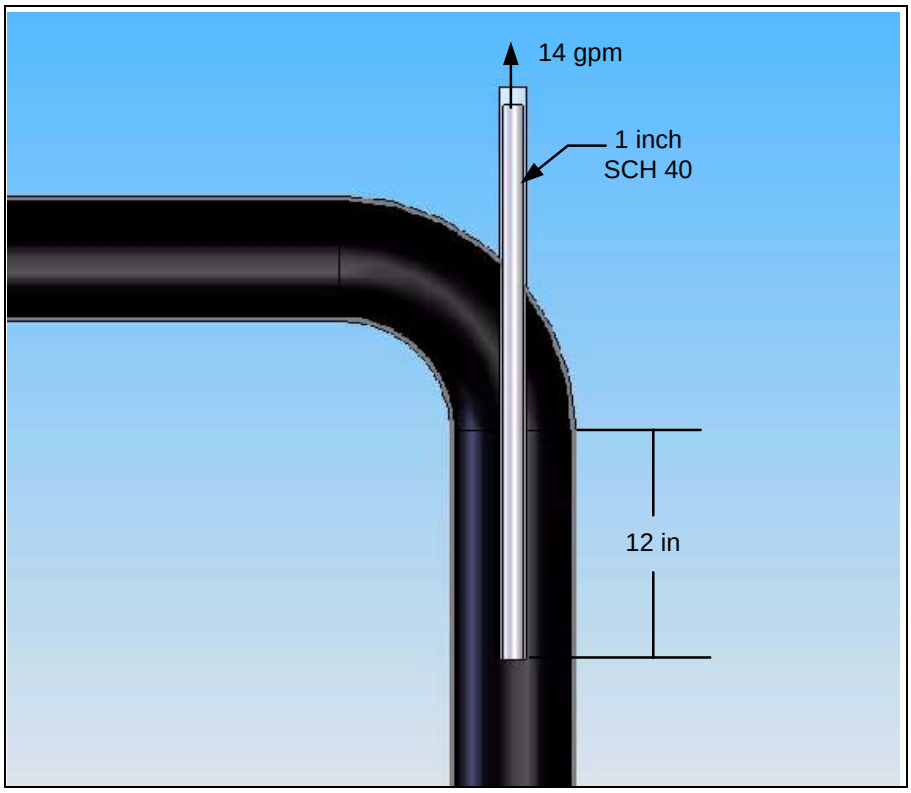

Figure 42. Sampling arrangement from last elbow.

The resulting trajectories and velocities along these trajectories for flow into the sample port are shown in Figure 43. There is a slight off-axis skewing of the flow into the port, due to the downstream piping and the lack of sufficient flow length in this downstream piping for fully developed flow. However, this skewing has no significant effect on the basic character of the flow into the port and the trajectories within the sample pipe. The sample flow has an entrance length of approximately two feet; therefore, the flow would be very close to fully developed before any flow-control device on the sample line.

Figure 44 shows the pressure distribution in the piping system near the sample port. The average pressure in the sample port was calculated to be 16.9 psi. Because this pressure is well above atmospheric pressure, no external pump would be required to induce sample flow. There would simply need to be a flow control on the sample line before the collection tank to maintain the desired 14-gpm flow rate.

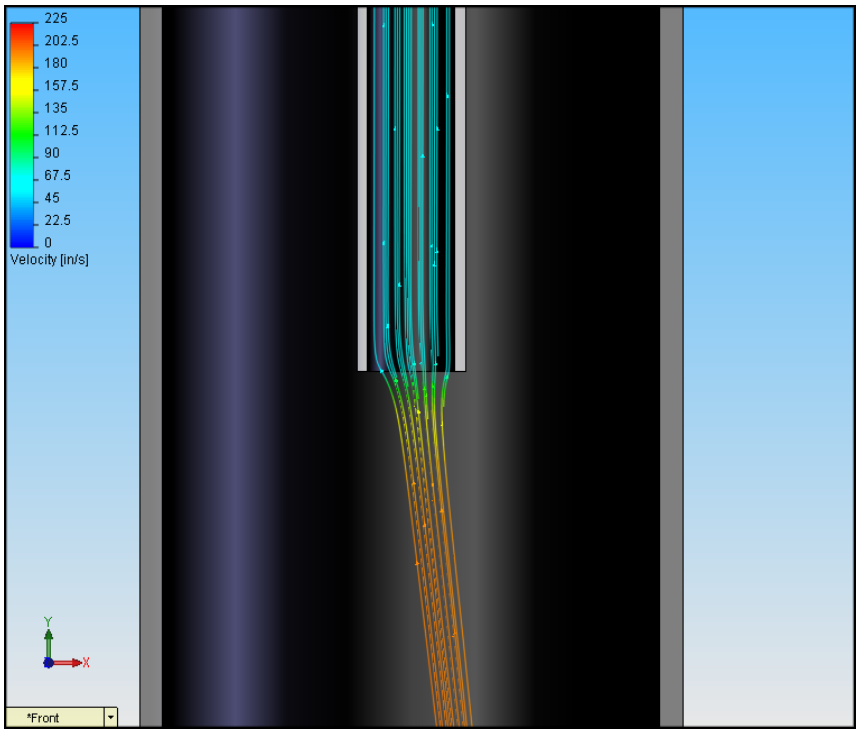

Figure 43. Flow trajectories into sample port.

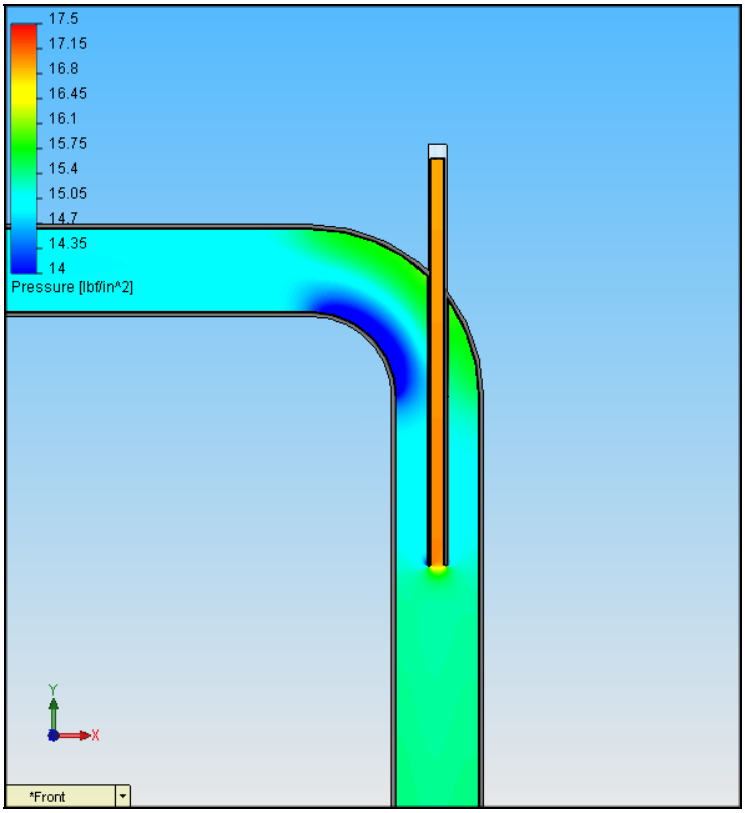

Figure 44. Pressure distribution.

6 CONCLUSIONS

The principal objective of this effort was to establish design and application guidelines for sampling biological organisms from ballast water systems. The primary goal of sampling is to extract a representative sample that minimizes adverse affects on sampled organisms. The results of the calculations and CFD simulations performed highlighted some of the differences between various sampler configurations and some of the potential problems.

One overarching conclusion from the particle studies is that particles, in this case simulating waterborne organisms, follow fluid flow trajectories and need not have their flow paths calculated separately. This is a direct result of the organisms having essentially the same density as seawater.

6.1 Isokinetic Sampling

Isokinetic sampling, where one attempts to match the velocity profile at the sample port to the velocity profile in the main piping, is the desired method of sampling multi-phase flows that can readily separate due to changes in velocity. Sampling for water content in oil is one classic example of this. However, as noted above, organisms in ballast water do not tend to separate from the flow trajectories; therefore, truly isokinetic sampling is not a requirement.

However, the isokinetic diameter calculation for the sample port does provide guidance for sizing the sample port. Simulations showed that flow transitions from the main stream were best for sample port diameters between 1.5 and 2.0 times the isokinetic diameter. Ports sized in this range had smooth transitions and pressure profiles that allowed for direct sampling without the need of a pump to induce sample collection.

6.2 Sampling Wand Design for Organisms

For the various port configurations considered, the following can be concluded:

- Tee port

  Tee ports have the distinct advantage of being simple to implement and low in cost. However, they have several drawbacks. Because they sample at the periphery of the pipe, most of the sample flow is from the main pipe's boundary layer. This periphery flow is subject to more interactions with the pipe walls; therefore, particles in this flow are more likely to impact the wall, which would likely result in organism mortality and/or degradation. The periphery of the pipe is also more likely to be the location of the extremes of particle distribution non-uniformity. Therefore, sampling with a tee is more likely to see a maximum or minimum of biological concentrations and would not be representative of the overall mean concentration.

Finally, the tee port does not have a smooth flow transition from the main pipe flow to the sampler exit. There is considerable narrowing of the flow to the downstream side of the sample port and a corresponding back eddy in the sample pipe. Although it is difficult to quantify the effect this would have on organism viability, it is assumed that a smooth transition from main pipe flow to sample flow reduces the risk of mortality.

- Extended tee

  The extended tee has most of the disadvantages of a simple tee sample port, with the additional problem of pressure drop. Because the tee is extended into the higher-velocity region of the pipe flow, Bernoulli's effect causes a significant drop in pressure at the entrance. In the simulations run for typical ballast water flows, this reduction in pressure was enough to require an external pump to extract the flow from the sample port.

  The extended tee does not suffer from sampling areas of non-uniform concentrations (and thus extreme high or low organism concentrations) that the simple tee does, because it samples from mid-stream of the flow. However, the transition from the main flow to the sample flow is even more problematic, with most of the flow sweeping down and very close to the sample port edge. This results in a more severe and potentially damaging environment for any organisms following this flow path.

- Straight extension elbows

  Sample ports with straight extensions facing upstream into the flow provided the best transition from the main flow to the sample piping. There was little noticeable difference in the flow pattern for extension lengths four times the sampler diameter or two times the sampler diameter. The initial redistribution of flow in the sample pipe occurs within approximately one diameter in length. This transition was smooth and would minimize any interaction with biological organisms and the sampler wall.

  Sampling at the centerline of the flow looking directly upstream can also be accomplished by inserting a straight sample pipe into a flange in an elbow of the main piping. This technique used for the shipboard example in Section 5, and is to be preferred, because it further simplifies the flow by eliminating the elbow.

- 45-degree cut elbow

  The 45-degree cut elbow showed no advantages over the elbow and had a distinctly poorer transition from the main flow to the sample pipe flow.

6.3 Sample Port Design and Installation Guidelines

The following guidelines pertain to sample port design and installation:

- Sample ports should be located as close to the overboard outlet as possible.
- Ideal sampling is from a long straight vertical pipe section.
- Sample with a straight-pipe section on the centerline of the main flow, looking into the flow.

- Sample port diameter should be between 1.5 and 2.0 times the basic isokinetic diameter.
- Sample port size should be based on the combination of maximum sample flow rate and minimum ballast flow rate that yields the largest isokinetic diameter.
- Ball valves should be used for shutting off the flow.
- Smooth-transition flow controls, such as flexible venturies, should be used to control flow rates.
- Piping and fittings from the sample port to the sample tank or strainer should be minimized.

7 REFERENCES

Fish, D. J. (1992). Isokinetic Crude Oil Sampling. *Pipe Line Industry*. Presented At Permian Basin Measurement Society Odessa, Texas, May 1997.

Henderson, C. B. (1976). Drag Coefficients of Spheres in Continuum and Rarefied Flows. *AIAA Journal*, v14, No. 6., 707–708.

Lemieux, E. J., Robbins, S., Riley, S., Cruz, D., & Hyland W. (2005). "Development of Methods for Biological Injections and Sampling from Fluid Lines", USCG RDC Final Report.

SolidWorks, Inc. (2005). COSMOSFloWorks® Fundamentals Manual, Chapter 2.1.

(This page intentionally left blank.)